Rapid leaf development drives the seasonal pattern of volatile organic compound (VOC) fluxes in a 'coppiced' bioenergy poplar plantation

TITLE

Rapid leaf development drives the seasonal pattern of volatile organic compound (VOC) fluxes in a 'coppiced' bioenergy poplar plantation

RUNNING TITLE:

Seasonality of VOC fluxes in coppiced poplars

Federico Brilli[*1,2,3], Beniamino Gioli[4], Silvano Fares[5], Zenone Terenzio[1], Donatella Zona[6], Bert Gielen[1], Francesco Loreto[3,7], Ivan A. Janssens[1] and Reinhart Ceulemans[1]

[1] Department of Biology, Centre of Excellence on Plant and Vegetation Ecology (PLECO), University of Antwerp, B-2610 Wilrijk, Belgium

[2] National Research Council, Institute of Agro-Environmental and Forest Biology (IBAF-CNR), Via Salaria Km 29,300 – 00016 Monterotondo Scalo, Roma, ITALY

[3] National Research Council, Institute for Sustainable Plant Protection (IPSP-CNR), Via Madonna del piano 10, 50017, Sesto Fiorentino, ITALY

[4] National Research Council, Biometeorology Institute (IBIMET-CNR), Via G. Caproni 8, 50145, Firenze, ITALY

[5] Council for Agricultural Research and Economics, Research Centre for the Soil-Plant System (RPS-CREA), Via della Navicella 2-4, 00184 Roma, ITALY

[6] Department of Animal and Plant Sciences, University of Sheffield, Western Bank – S10 2TN, Sheffield, UK

[7] National Research Council, Department of Biology, Agriculture and Food Sciences (CNR-DISBA), P.le Aldo Moro, 00185 Roma, ITALY

*Corresponding author presently at:

National Research Council, Institute of Agro-Environmental and Forest Biology (IBAF-CNR), Via Salaria Km 29,300 – 00016 Monterotondo Scalo, Roma, ITALY

Tel.: +39 06 90672535

Fax: + 39 06 9064492

Email: federico.brilli@ibaf.cnr.it

This article has been accepted for publication and undergone full peer review but has not been through the copyediting, typesetting, pagination and proofreading process which may lead to differences between this version and the Version of Record. Please cite this article as doi: 10.1111/pce.12638

ABSTRACT

Leaves of fast-growing, woody bioenergy crops often emit volatile organic compounds (VOC). Some reactive VOC (especially isoprene) play a key role in climate forcing and may negatively affect local air quality. We monitored the seasonal exchange of VOC using the eddy covariance technique in a 'coppiced' poplar plantation. The complex interactions of VOC fluxes with climatic and physiological variables were also explored by using an artificial neural network (Self Organizing Map). Isoprene and methanol were the most abundant VOC emitted by the plantation. Rapid development of the canopy (and thus of the Leaf Area Index, LAI) was associated with high methanol emissions and high rates of gross primary production (GPP) since the beginning of the growing season, while the onset of isoprene emission was delayed. The highest emissions of isoprene, and of isoprene photoxidation products (Methyl Vinyl Ketone and Methacrolein, i_{ox}), occurred on the hottest and sunniest days, when GPP and evapotranspiration were highest, and formaldehyde was significantly deposited. Canopy senescence enhanced the exchange of oxygenated VOC. The accuracy of methanol and isoprene emission simulations with the MEGAN model increased by applying a function to modify their basal emission factors, accounting for seasonality of GPP or LAI.

KEYWORD INDEX

VOC, fluxes, LAI, *Populus*, SOM, MEGAN, bioenergy

INTRODUCTION

Future increasing demand for bioenergy implies aggressive expansion of biomass-based energy sources (Özdemir et al. 2009; IPCC 2011; Energy Information Administration 2013). Consequently, large-scale widespread cultivation of feedstock crops for bioenergy will progressively replace native agricultural crops and natural ecosystems determining significant land use changes (Searchinger et al. 2008; Koh et al. 2009).

Herbaceous and fast-growing woody crops are selected as candidates for bioenergy feedstock because biomass accumulation is enhanced by the combination of high photosynthetic rates (Weih et al. 2004; Calfapietra et al. 2010) and fast development of leaf area index (LAI) (Broeckx et al. 2012), especially when plants are intensively grown in short rotation 'coppice' culture (SRC). Leaves of many plants emit volatile organic compounds (VOC) (Kesselmeier & Staudt, 1999; Loreto et al. 2014). The magnitude and the chemical composition of VOC emissions are species-specific, but most of the herbaceous shrubs and woody bioenergy crops are high isoprene emitters (Porter et al., 2012; Guidolotti et al. 2011; Loreto & Fineschi, 2015).

Isoprene (2-metyl-1,3-butadiene) plays a key role in present and future climate forcing (Shallcross & Monk, 2000; Collins et al. 2002) because it is involved in photochemical reactions leading to the formation of tropospheric ozone (Chameides et al. 1988) and aerosols (Claeys et al. 2004; Carlton et al. 2009). Therefore, the widespread establishment of isoprene-emitting bioenergy crops may negatively impact on local air quality (Ashworth et al. 2012; Porter et al. 2012; Beltman et al. 2013) with possible consequences on human health (Ashworth et al. 2013; Porter et al. 2015). Moreover, since isoprene protects leaves against the occurrence of oxidative and thermal stresses (Vickers et al. 2009, Loreto & Schnitzler 2010) and mediate plant-insect-interactions (Loivamäki et al. 2008; Laothawornkitkul et al. 2008), large land-use changes derived from intensive bioenergy production may have

unpredictable consequences on ecological adaptation and diversity (Dionigi et al. 2010; Miresmailli et al. 2013).

Besides being species-specific, the amount and type of constitutive VOC emissions strongly depend on leaf age and plant developmental stage. Isoprene is mainly emitted by adult, fully expanded leaves (Hakola et al. 1998; Brilli et al. 2009), but methanol is released at high rates in young developing leaves, mainly as a by-product of pectin methylesterase (PME) enzymatic activity in expanding cell walls (Gaffe et al. 1994; Oikawa et al. 2011a). Methanol may have a signaling role in plants interacting with herbivores (Von Dahl et al. 2006). Although methanol is not as reactive as isoprene (Jacob et al. 2005), it affects the chemistry of the upper troposphere by modulating the presence of hydroxyl ($^{\bullet}$OH) radicals (Tie et al. 2003) and may also interact locally with air quality, being a source of formaldehyde (Palmer et al. 2003).

Methanol and isoprene are subject to different physiological and physico-chemical controls (Niinemets et al. 2004), and thus exhibit a pronounced, but distinct, temporal variability over short time scales (Brilli et al. 2014). While isoprene production and emission rates are mainly controlled by both temperature and light intensity (Loreto & Sharkey, 1990), methanol biosynthesis is related mostly to plant growth, which responds to changes in temperature, but is less affected by light (Oikawa et al. 2010a, b). Higher temperatures and more energy are required for the enzymatic activity of isoprene synthase (IspS) than of PME (Rasulov et al. 2014; Oikawa et al. 2010a). In addition, the lower gas/water partition coefficient (higher solubility in water) makes methanol (and other oxygenated water soluble VOC, such as formaldehyde) more storable in foliar water pools (Niinemets et al. 2004).

Long-term changes of VOC emissions are regulated by the response to environmental variables (i.e. light intensity, or photosynthetically active radiation, PAR; air temperature, Tair; vapor pressure deficit, VPD) and by the seasonal variations of plant physiological

factors (i.e. gross primary production, GPP; stomatal conductance; and transpiration, ET) which are in turn also dependent on characteristics of the canopy structure (i.e. leaf area index, LAI). All these drivers affect isoprene (Monson et al. 1994; Brüggemann et al. 2002; Rasulov et al. 2015; Wiberley et al. 2008) differently from methanol (Hüve et al. 2007) and other VOC (Park et al. 2013). However, simple relationships between VOC fluxes and a single environmental variable do not represent the real complex interactions (also involving physiological processes and canopy structure) determining VOC emission and deposition. Different from process models, an observation-driven methodology, based on an artificial neural network (i.e. Self-Organizing Map, SOM) (Kohonen et al. 2001), might be a useful statistical methodology to explore and visualize effectively the multivariate relationships existing between the long time-series of climatic, physiological, and canopy structural variables, and (bidirectional) fluxes of many VOC.

Seasonal patterns of VOC fluxes are most often simulated using the canopy-scale model of emissions of gases and aerosols from nature (MEGAN; Sindelarova et al. 2014). Compared to the original model formulation based on foliar scale processes (Guenther et al. 1995), MEGAN has recently been improved into a multi-layer canopy model to reproduce the dynamics of light extinction and changes in temperature within a canopy, and to include variations of age-dependent leaf emissions, based on LAI development (Guenther et al. 2012). However, this improved version of MEGAN does not account properly for the seasonal variation of the enzymatic activity regulating the basal emission factor (BEF) employed in the model (Schnitzler et al. 1997). Enzyme activities may largely influence VOC emissions, especially in coppiced plantations characterized by a large amount of juvenile developing leaves for most the season. Furthermore, the seasonal variability in the BEF of isoprene emission was found to strongly correlate with the seasonality of GPP (Kuhn et al. 2004). Thus, a correction of BEF to account for the changes in GPP may be used to increase

the simulation accuracy of long-term changes in the emission capacity. The simulated exchange of VOC by bioenergy crops has often been validated with scarce empirical data collected in the field, for short periods of time (Misztal et al. 2011; Porter et al. 2012).

So far, projections of large-scale land use changes associated with cultivation of bioenergy crops mostly considered the energy requirements and the exchange of greenhouse gasses (i.e. CO_2) (Ou et al. 2009; Gelfand et al. 2011). Comprehensive investigation of the seasonal pattern of VOC emission profiles in bioenergy crops has been carried out only for some herbaceous plant species (Eller et al. 2011; Graus et al. 2012; Miresmailli et al. 2013) and only for an evergreen, broad-leaved ecosystem characterized by a limited seasonal variation of LAI (oil palm plantation, Misztal et al. 2011).

Because of the expanding use of isoprene-emitting poplars (*Populus spp.*) as bioenergy crops (Cai et al. 2011), a continuous, seasonal study of the exchanges of VOC above a 'coppiced' poplar plantation having rapid seasonal variation of LAI is highly demanded. Indeed, in poplars growing in SRC plantation, high photosynthetic rates (Dillen et al. 2011; Weih et al. 2004) are sustained by large and prolonged stomatal opening. Open stomata allow considerable bidirectional fluxes of gases between the leaf mesophyll and the atmosphere (Niinemets et al. 2014; Fares et al. 2015) when growth is not limited by environmental constraints (Migliavacca et al. 2009; King et al. 2013; Pita et al. 2013).

Here we present the results of an intensive field campaign where the exchanges of VOC, CO_2, and water vapor were continuously monitored during an entire growing season (from June to November) above a poplar plantation resprouting from coppiced stools. In this study, we report: (a) the dynamics of emission and deposition fluxes of a multitude of VOC over a growing season; (b) the relationships between VOC emission/deposition fluxes and the seasonal variations of potential environmental (PAR, Tair, VPD) and physiological (GPP;

NEE, ET) drivers also including canopy structural traits (LAI); (c) the total amount of carbon either deposited or emitted in the form of VOC; (d) the performance of the canopy-scale MEGAN emission model when tested with long time-series of isoprene and methanol flux measurements. In particular, we verified whether the simulation accuracy of MEGAN could be increased by modifying the BEF to account for the seasonal changes of two physiological factors potentially responsible for the variable BEF performances, such as GPP and LAI.

MATERIALS AND METHODS

Field site description

The research site (http://uahost.uantwerpen.be/popfull/) was located in Lochristi (51° 04'44'' N, 3°51'02'' E; Belgium) at an elevation of 6 m a.s.l. in a completely flat terrain. A multi-genotype poplar (*Populus spp.*) short rotation coppice (SRC) plantation was established in April 2010 and coppiced in January-February 2012 at the end of a first two-year rotation. Planting density was 8000 plants ha^{-1} and the planting layout consisted of a double-row design. After coppicing, many new shoots re-sprouted per stool at the end of May (Fig. S1a) and continued to grow until November (2012), when the canopy began yellowing and shedding leaves (Fig. S1f) (Zenone et al. 2015). The plantation was neither irrigated nor fertilized. More detailed descriptions of field site and plantation management were published previously (Broeckx et al. 2012; Verlinden et al. 2015; Zona et al. 2012; 2013).

Eddy covariance flux measurements and quality control

The site was equipped with two complete and independent monitoring systems for eddy covariance (EC), installed on the same meteorological mast. The first EC system, consisting of a closed-path infrared gas analyzer (LI-7000, LI-COR, Lincoln, NE, USA) coupled with a sonic anemometer (CSAT-1, Campbell Scientific Inc., Logan, UT, USA), was installed for

CO_2 and H_2O flux measurements. The second EC system, including a sonic anemometer (model USA1, Metek GmbH, Elmshorn, Germany) coupled with a Proton Transfer Reaction "Time-of-Flight" Mass Spectrometer (PTR–TOF–MS, Ionicon, Innsbruck, Austria), was set up for VOC flux measurements, as described in detail by Brilli et al. (2014).

Multiple VOC were detected by the PTR–TOF–MS through proton transfer reactions occurring between the H_3O^+ ions and the air sample injected into a drift tube under constant ionization energy conditions (E/N of ~ 120 Td). After extraction from the drift tube, protonated ions were pulsed and separated according to their mass-to-charge (*m/z*) ratio (Jordan et al. 2009; Graus et al. 2010). Raw high-resolved full mass spectra of protonated ions (up to *m/z* of 315) were continuously acquired at high frequency (10 Hz) by the TofDaq software (Tofwerk AG, Switzerland) between June 4 and October 31, 2012, corresponding to day of the year (DOY) 156 to 305. To reduce the burden of PTR-TOF-MS data analysis, the overall raw dataset collected during the measuring campaign was post-processed by the routine programs of Müller et al. (2013) and normalized to account for the water dependency of the PTR-TOF-MS sensitivity. This allowed us to screen for the presence of emitted/deposited fluxes of the most common protonated ions (Tab. 1, Tab. S2) which were unambiguously related to VOC, either as molecular ions, or as their fragments (Holzinger et al. 2010; Brilli et al. 2012, 2014; Park et al. 2013). After post-processing, PTR-TOF-MS data were background corrected by subtracting emissions measured in VOC-free air, generated by a gas calibration unit (GCU) (Ionimed, Innsbruck, Austria), and regularly calibrated with the same gas standard (Apel Riemer, USA) during the entire field campaign (Tab. S3). The use of gas standards also allowed us to quantify the volume mixing ratios (VMRs) of the selected VOC (Fig. S3), as described previously (Brilli et al. 2014).

Half-hourly fluxes of CO_2 and water vapor were computed by using the EddyPro software (www.licor.com/eddypro, Fratini et al. 2012). A customized version of EddyPro, named

EddyVOC (developed by Brilli et al. 2014) standardized the computation of a multitude of VOC fluxes. A quality control was applied to all half-hourly fluxes according to Göckede et al. (2004). In addition, a friction velocity (u*) = 0.12 m s^{-1} was estimated when the dependence of the nighttime NEE on friction velocity reached saturation and used as a threshold below which data were discharged. Here positive fluxes represent transport of gases from the canopy toward the atmosphere (emissions), while negative fluxes represent gas depositions.

Gap filling of CO_2 and VOC fluxes

Measurements were successfully collected for more than 90% of the time, interrupted by only few technical failures and routine instrument maintenance and calibrations. The time series of the CO_2 fluxes was gap-filled and then partitioned into ecosystem respiration (RECO) and GPP by using the marginal distribution sampling (MDS) method (Reichstein et al. 2005) according to Moffat et al. (2007) and Papale et al. (2006). In particular, the regression model of Lloyd & Taylor (1994) was used to derive RECO from NEE and then GPP was calculated as:

$$GPP = |NEE| + RECO \quad (1)$$

Missing half-hourly VOC flux data were gap filled by using the mean diurnal variation (MDV) as proposed by Bamberger et al. (2014). According to this method, missing data were replaced by the corresponding values of the average diurnal cycle calculated within a time window of ± 8 days around the missing values.

Ancillary data

Meteorological parameters were continuously recorded during the experimental period, and data were stored on different data loggers (model CR3000, CR5000 and CR1000; Campbell

Scientific, Logan, Utah, USA). Incoming PAR was measured above the canopy using a quantum sensor (Li-190; LI-COR, Lincoln, NE, USA). Air temperature (Tair) and relative humidity (RH) were monitored by using a Vaisala probe (model HMP45C, Vaisala, Helsinki, Finland) at 6 meters height on the EC mast while vapor pressure deficit between leaves and the air (VPD) was derived from Tair and RH measurements. Volumetric soil water content (SWC) was assessed at 0.2-m depth by time domain reflectrometry (TDR model CS616; Campbell Scientific, Logan UT, USA). Discrete measurements of LAI were collected in the field during different measurement campaigns (Fig. S1) as described by Broeckx et al. (2015). Best-fitting regression applied to the measurements of LAI yielded an equation (2) (below) (R^2 = 0.96, $p < 0.001$) which was used to obtain a continuous time-series of LAI values (Fig. S2h) with SigmaPlot version 11.0 (Systat Software Inc., San Jose, CA, USA):

$$f(x) = a * f(x) = e^{\left[-0.5*\left(\frac{(X-X0)}{b}\right)^2\right]} \quad (2)$$

where a (= 5.54 ± 0.17) and b (= 44.7 ± 1.86) are fitting parameters, x and x_0 refer to the time interval.

Self Organizing Map (SOM)

The Self Organizing Map (SOM) is an artificial neural network that projects complex, non-linear statistical relationships between high-dimensional data into simple geometric relationships on a regular two-dimensional component plane (Kohonen, 2001; Oja et al. 2003). In this work, SOM was used to explore and visualize in the same figure (Fig. 2) all the relationships between full time-series of (bidirectional) VOC fluxes and environmental (Tair, PAR, VPD) and physiological variables (GPP, NEE, RECO, ET) also including traits of canopy structure (LAI). Panels shown in Fig. 2 are component planes of the SOM.

Differently from other data mining tools, SOM is an unsupervised nonparametric approach, meaning that it does not have any category information to elaborate the data. Moreover, a clear advantage with respect to traditional statistical methods is that SOM does not need to have prior hypotheses to be confirmed. SOM was here applied to cluster various half-hourly data on two-dimensional component planes, and not to explain the variance of the data. Each given half-hourly data received a single location on a component plane and similar data received locations near each other on the same component plane according to the SOM training algorithm (Kohonen, 2001). Importantly, across all different component planes, half-hourly measurement of VOC fluxes and variables collected at the same time are always located in the same point. In each component plane of Fig. 2, the intensity of either one flux or a variable is represented with color-coding. Hence, either similar or contrasting intensities of VOC fluxes can be compared with values of environmental and physiological variables by looking at exactly the same area within the component planes. In other words, by using the position and coloring, relationships between different (emission and deposition) fluxes of VOC and either environmental or physiological variables including LAI can be easily explored, (i.e.) the highest VOC emission (or deposition) rates and the highest (or lowest) values recorded for all variables will be clustered and visualized by the same colour and, if a correlation occurred between fluxes and variables, the coloured space will be located in the same area within the different component planes.

The best fit of the model used to create SOM was measured with a topographic error (Kiviluoto, 1996) that was only 9.3 % after processing our dataset. Because of the low percentage of topographic error, the topology of the dataset was well preserved during the SOM elaboration. More details on the SOM application can be found in Luyssaert et al. (2007).

Model of Emissions of Gases and Aerosols from Nature (MEGAN): inputs and parameters

Emissions of VOC (*E*, nmol m^{-2} s^{-1}) were calculated according to equation (3) as described in Guenther et al. (2012) with a model algorithm parameterized with PAR and Tair:

$$E = BEF \cdot \gamma \cdot \Delta \cdot LAI \cdot CE \quad (3)$$

where basal emission factor (BEF) is calculated at a fixed standard PAR and Tair (Guenther et al. 1995), LAI is the leaf area index (see above), CE (= 0.57) is a constant that sets the emission activity to unity at standard conditions for the MEGAN model and γ is an emission activity factor that account for emission changes due to the variations of light and temperature from standard conditions.

Similarly to Misztal et al. (2011) and Fares et al. (2013), γ was calculated according to equation (4):

$$\gamma = b_3 \cdot \exp[b_2 \cdot (P_{24} - P_0)] \cdot (P_{24})^{0,6} \cdot \frac{[b_1 - b_2 \cdot \ln(P_{240})] \cdot PAR}{\sqrt{1 + [b_1 - b_2 \ln(P_{240})]^2 \cdot PAR^2}} \cdot b_5 \cdot \exp[b_6 \cdot (T_{24} - 297)]$$

$$\cdot b_5 \cdot \exp[b_6 \cdot (T_{24} - 297)] \cdot \exp[b_6 \cdot (T_{240} - 297)] \cdot \frac{C_{T2} \cdot \exp\left[C_{T1} \cdot \left(\frac{1}{T_{opt}}\right) - \left(\frac{1}{T}\right) \cdot \frac{1}{0.00831}\right]}{C_{T2} - C_{T1} \cdot \left[1 - \exp\left(C_{T2} \cdot \left(\frac{1}{T_{opt}}\right) - \left(\frac{1}{T}\right) \cdot \frac{1}{0.00831}\right)\right]} \quad (4)$$

where the first line of equation (4) represents the PAR effects, while the second equation line represents the effects of Tair.

Differently from the original formulation, we did not apply a soil moisture function. Soil moisture was not a limiting factor in our plantation as there were frequent rain events during the measurement campaign never caused the SWC to drop (Fig. S2h).

In a first model simulation, we tested a constant value of BEF for isoprene (= 10.9 nmol m^{-2} s^{-1}) obtained directly from leaf enclosure measurements at the site (Brilli et al. 2014). A constant BEF of 10.0 nmol m^{-2} s^{-1} was assigned to methanol according to previous profile measurements on poplars (Fares et al. 2010), due to the impossibility of measuring methanol with leaf enclosures in the field using the same analytical instrumentation employed for isoprene. In a second simulation, dynamic values of BEF were obtained for both methanol and isoprene by adjusting the constant values given above, on the basis of the seasonal time-course of either LAI or GPP (Fig. S4). In brief, BEF was multiplied by Δ, a factor (ranging between 0-1) that normalizes the BEF for the effects of seasonality, as recently proposed by Kemper-Pacheco et al. (2014). Δ was calculated either on the basis of the seasonality of LAI obtained from equation (2) or on the basis of the seasonality of GPP according to equation (5):

$$\Delta = e^{\left[-0.5*\left(\frac{(DOY-230)}{43.4}\right)^2\right]} \quad (5)$$

Modelled fluxes were correlated with measured observations, and linear correlations (R^2), root mean squared error (RMSE) and Akaike information criterion (AIC) values were calculated with SigmaPlot version 11.0 (Systat Software Inc., San Jose, CA, USA).

RESULTS

VOC fluxes

Isoprene (*m/z* = 69.069) and methanol (*m/z* 33.033) were the most abundant trace gases emitted by the plantation over the course of the growing season (Fig. 1; Tab. 1). Methanol emission did not show a clear seasonal trend. High emissions of methanol (> 5 nmol m^{-2} s^{-1}) were measured already in June (Fig. 1b), but the highest emission occurred in mid-August (~19 nmol m^{-2} s^{-1}) (Tab. 1). The onset of isoprene emission was delayed with respect to methanol (Fig. 1g) and displayed a clearer seasonal trend, with a gradual increase starting from the end of July, a peak in mid-August (~40 nmol m^{-2} s^{-1}; Fig 1g), before dropping in September, concurrent with decreasing Tair (Fig. S2a). The mid-August peak in isoprene fluxes corresponded to minimum NEE, maximum GPP and LAI values (Fig. S2e, h), and maximum Tair.

The season-long measurements showed mean (-0.01 nmol m^{-2} s^{-1}) and median (-0.10 nmol m^{-2} s^{-1}) deposition fluxes at *m/z* = 31.018, assigned to formaldehyde (Fig. 1a; Tab. 1). Possible interferences of other ions (i.e. methyl peroxides) confounding the formaldehyde signal at *m/z* 31.018 were negligible in our study, as indicated by the constant deposition velocity of *m/z* 31.018 during the central hours of the day (data not shown). A bidirectional exchange of other oxygenated VOC was also found (Tab. 1). These included aldehydes (acetaldehyde *m/z* = 45.033 and a fragment of hexanaldehyde *m/z* = 83.085) (Fig. 1c, k), ketones (acetone *m/z* = 59.049 and methyl ethyl ketone - MEK *m/z* = 73.068) (Fig. 1f, i), organic acids (formic acid *m/z* = 47.012 and propionic acid *m/z* = 75.043), (Fig. 1d, j), and isoprene oxidation products as methyl vinyl ketone and methacrolein (MVK and MAC together referred as i_{ox}, *m/z* = 71.049) (Fig. 1h). Other isoprenoids (i.e. monoterpenes detected as both protonated ion fragment *m/z* = 81.070 and as protonated molecular ion *m/z* = 137.133) were occasionally released from the poplar plantation during the season (Fig. 1k, l; Tab. 1).

Relationships between VOC fluxes, environmental and physiological parameters

The SOM explored and visualized in one single snapshot (Fig. 2) all the complex temporal relationships occurring between the half-hourly fluxes of the main VOC emitted by the plantation (Fig. 1) and the aggregated climatic factors (half-hourly Tair, PAR, VPD) (Fig. S2a, c), and physiological processes (half-hourly NEE, GPP, RECO, ET) (Fig. S2d, e, f, g), also including canopy structural traits (half-hourly LAI) (Fig. S2h) collected during the entire measurement season. On the SOM planes referring to VOC fluxes (Fig. 2a-l), the highest emission rates are represented by dark red whereas the highest deposition rates are represented by dark blue. On the SOM planes referring to all physiological (Fig. 2m-p), environmental (Fig. 2q-s), and structural (Fig. 2t) variables the lowest measured values are dark blue and the highest values are dark red.

The most abundant emissions of isoprene and methanol occurred on the warmest days, under mid to high PAR, when NEE reached the lowest (and GPP the highest) rates in combination with maximum ET values (Fig. 2b, g, m, n, p, q, r; bottom-left corner of the different component planes). Regression analysis confirmed the relationship between both methanol and isoprene emissions with GPP (Fig. 3g, h; Tab. 2).

However, while isoprene emission is light- and temperature-dependent (Fig. 3b, d; Tab. 2), methanol resulted almost insensitive to variations of both PAR and Tair over the season (Fig. 3a, c; Tab. 2). This confirmed a different regulation of the biosynthesis of isoprene with respect to methanol. Both the dependencies of isoprene emission on PAR and Tair decreased progressively between June and August, most likely because of acclimation. However, in September as LAI decreased and senescence had started (Fig S1e; S2h), PAR and Tair dependencies of isoprene emission were as high as in July, and then dropped in October (Fig. 3b, d; Tab. 2). High isoprene emissions were only associated with high values of LAI (bottom-left corner of the different component planes of Fig. 2g, t). Whereas, high methanol

emissions were associated to high VPD and high ET, which could be explained by the high stomatal conductance of leaves exposed to high temperature and light levels (bottom-left area of the different component planes of Fig. 2b, n, q, r, s). The relationship between methanol emission and ET was further confirmed by our study, and appeared to remain constant over the season (Fig. 3i; Tab. 2). Due to its high solubility in water, part of methanol temporarily stored in the cellular aqueous solution can be readily volatilized also under high VPD and intermediate ET levels (central area of the different component planes of Fig. 2b, n, s). Likewise methanol, isoprene is a low molecular weight VOC having high vapor pressure and thus high isoprene emissions were also associated to high VPD (and Tair) (Fig. 2g, r, s). Moreover, high isoprene emissions were also related to high ET (bottom-left area of the different component planes of Fig. 2g, n, q, r, s) when leaves actively transpire through opened stomata. The relationship between ET and isoprene emissions was stronger than between ET and methanol (Tab. 2).

The SOM also confirmed that other isoprenoids (i.e. monoterpenes) were emitted, as isoprene, (Fig. 2g, j, l) under high (Fig. 2g, j, l, q, r; bottom-centrum of the different component planes) or intermediate (Fig. 2g, j, l, q, r; central-left area of the different component planes) Tair and PAR levels.

The bidirectional exchange of oxygenated VOC (i.e. formaldehyde, acetaldehyde, acetone, formic acid, ethanol, GLV fragments) was also analyzed by SOM (Fig. 2). SOM revealed that peak emissions of all the oxygenated VOC, irrespective on their (daily or seasonal) variation, occurred together, especially when LAI values were very low (Fig. 2a, c, d, e, f, j, k, t; right side and bottom-right corner of the different component planes) i.e. during senescence, at the end of the season (Fig 1). Emissions of isoprene oxidation products (i_{ox}) and MEK were observed when isoprene production was highest and photochemical reactions were promoted, i.e. under the warmest and sunniest conditions (Fig. 2h, i, q, r; bottom-central area of the

different component planes). Last, the SOM indicated that conditions of high PAR, Tair, VPD and ET (Fig. 2a, n, q, r, s; bottom-central area of the different component planes) also favored deposition of formaldehyde.

Seasonal VOC fluxes and carbon budgets

After filling data gaps in the VOC flux measurements and subtracting deposited from emitted VOC, the plantation was found to be a net, albeit very small (~1 g m^{-2} growing season $^{-1}$) VOC carbon source to the atmosphere (Fig. 4; Tab. 3). Carbon fixed into VOC, was mainly emitted from the poplar plantation as isoprene (0.791 g C m^{-2} growing season $^{-1}$) and methanol (0.144 g C m^{-2} growing season $^{-1}$). Carbon emissions in the form of acetone (0.017 g C m^{-2} growing season $^{-1}$) and of a GLV fragment (0.013 g C m^{-2} growing season $^{-1}$) were much lower, but still an order of magnitude higher than emissions of all other VOC (Tab. 3).

When breaking down observations along the season, a minimal amount of carbon in the form of VOC (< 0.01 g C m^{-2} day) was daily taken up by the growing plantation (Fig. 4b). However, only formaldehyde showed net deposition, albeit very limited over the entire length of the season (Tab. 3). Daily emissions of carbon in the form of VOC showed a much stronger seasonal variation than daily deposition (Fig. 4b), with a peak at the end of June, rapidly increasing fluxes at the end of July, and a higher peak in mid-August, followed by a steady decline.

The temperate oceanic climate of Belgium was characterized by relatively warm (but never hot) summertime temperatures (Fig. S2a) coupled with frequent precipitations that kept the SWC level quite stable over the season and prevented drought episodes (Fig. S2h). These conditions did not limit the development of LAI and GPP, both of which increased following a similar trend from June to September (Fig. 4a, d; Fig. S4). In September, the rise of NEE above zero (GPP being less than RECO), was coupled with reduced LAI values, indicating

the onset of leaf senescence (Fig. 4a, d). Similarly, from June to September, the progressive rise of carbon emitted as VOC mirrored the exponential development of LAI (Fig. 4d). When senescence approached in September-October, LAI values decreased as leaves started to fall, causing no further increase in the cumulative emission of VOC (Fig. 4d). Overall, the total amount of VOC emitted during the entire growing season accounted for only 0.07% of the carbon uptake through GPP and 0.8% of the ecosystem NEE (Tab. 2).

Performance of MEGAN model

The simulated time-course of daily methanol and isoprene emissions provided a good fit with the observed values, especially when a dynamic (rather than a constant) BEF was applied to account for the seasonality of the photosynthetic capacity (indicated by changes in GPP rates) or the rapid development of a canopy (indicated by the increase of LAI). Indeed, changes of these two physiological factors (GPP and LAI) might have particularly affected the changes of isoprene and methanol emission capacity over the season in a 'coppiced' plantation. (Fig. 4). This was further demonstrated by the lower Akaike information criterion (AIC) values obtained from simulations with a dynamic rather than a constant BEF (Tab. 4). Irrespective of whether a constant or a dynamic value of BEF was applied, MEGAN performed better for isoprene than for methanol (Tab. 4) most likely because of a different regulation in the two emissions.

However, rising emissions were overestimated in both model simulations during fast Tair increases occurring in two episodes, at the end of July and near the middle of August (Fig. 5a, c; Fig. S2a). In particular, simulated methanol emissions were overestimated to a similar extent in the two episodes (Fig. 5a), but the difference between simulated and measured isoprene emissions was only higher at the end of July (Fig. 5c). Estimation of the cumulative sum of carbon emitted as methanol was more reliable when a LAI-dependent dynamic BEF

was applied to MEGAN (Fig. 5b; Tab. 4). Moreover, the total carbon emitted as isoprene was estimated more properly when the dynamic BEF was fitted to GPP (Fig. 5d; Tab 4).

DISCUSSION

This study reports VOC emissions from a re-sprouting poplar plantation after coppicing, a common practice in agro-forestry, and especially when growing biomass/bioenergy crops. In contrast to poplar stands in a Mediterranean climate (Migliavacca et al. 2009) or to an old aspen forest in North-America (Fuentes et al. 1999), the growth period of this temperate coppiced poplar plantation was restricted to the summer months only (early June to mid-September). Such a limited growth period was shorter than the previous (Zona et al. 2013) and the following years (Zenone et al. 2015), but similar to that of poplars growing at mid- and high-elevation sites (Monson et al. 1994).

Emissions of isoprene and methanol were the highest among the multitude of VOC recorded in the present study, and should be considered constitutive, as neither abiotic nor biotic stresses were experienced by the plantation during the measurement period. Indeed, emissions of specific VOC induced by drought (Karl et al. 2008) or insect herbivory (Van Poecke et al. 2001; Brilli et al. 2009) e.g. GLVs (Tab. 1), sesquiterpenes, methyl salicylate (MeSa) and methyl jasmonate (MeJa) were negligible throughout the experiment (Tab. S1).

The rapid canopy (and thus LAI) development induced high rates of methanol emission since the beginning of the growing season, early in June. Indeed a very fast growth of poplar shoots from the coppiced stumps occurred along with a swift increase of LAI (from 0 to 5.60 ± 1.36) until the end of August (Fig S2h). These observations confirmed high emissions of methanol in juvenile expanding poplar leaves under controlled laboratory conditions (Hüve et al. 2007; Fares et al. 2010). Moreover, the good agreement between ecosystem level methanol emission rates and canopy development, together with near-zero fluxes commonly observed

during nighttime when stomata are almost fully closed, indirectly suggests that additional multiple sources of methanol within the ecosystem (e.g. soil, plant, bacteria; Penuelas et al. 2014) did not significantly contribute to methanol flux (Asensio et al. 2007; Peñuelas et al. 2014). In fact, the magnitude of methanol emission was similar to those measured in different ecosystems (Wohlfahrt et al. 2015), but much higher than those of evergreen citrus orchards (Fares et al. 2012), tropical rainforests (Langford et al. 2010), oil palm plantations (Misztal et al. 2011), or coniferous forests (Schade et al. 2011). Possibly, sustained rates of methanol emission reflected fast development of the canopy in coppiced poplars. Our study confirmed the relationship found between methanol fluxes and GPP during the season (Fig. 2b, p; Fig. 3g; Tab. 2) (Galbally & Kristine, 2002; Wohlfahrt et al. 2015). However, our SOM-based exploratory data analysis highlighted a more complex relationship also involving the variability of Tair and VPD as important factors in regulating methanol emissions (Fig. 2b, r, s). In fact, both Tair and VPD affect stomatal opening (Niinemets & Reichstein, 2003) and alter the degree of methanol solubility and storage in aqueous pools within the plant (Niinemets et al. 2004). This likely explains the high methanol emissions from open stomata that transpire at high rates during active growth in wet and temperate oceanic climate regions of North-Western Europe. Consistent with previous studies (Mistzal et al. 2011; Schade et al. 2011; Laffineur et al. 2012; Park et al. 2014) our results showed bidirectional exchanges of methanol, although the total amount of carbon deposited in the form of methanol accounted for only 10% of that emitted (Tab. 3). Atmospheric deposition of methanol may occur through processes of adsorption/dissolution in water films on the canopy or in the soil (Laffineur et al. 2012), as well as through catabolic pathways present in plants (Gout et al. 2000) and in methylotrophic bacteria (Fall & Benson, 1996). Methanol is ubiquitously produced in plants as a by-product of PME enzymatic activity during growth and expansion of leaves (Nemecek-Marshall et al. 1995; Fall & Benson, 1996; Loreto et al. 2006). Although

substrate limitations to methanol production are still a matter of debate (Oikawa et al. 2011a), large emissions from different ecosystems (Wohlfahrt et al. 2015) indicate a broad range of optimal temperature for PME enzymatic activity. High PME activity was found in both juvenile and mature leaves (Oikawa et al. 2011a) and we confirmed (Fig. 3a; Tab. 2) methanol emission to be weakly sensitive to variation of light (Oikawa et al. 2011b; Brilli et al. 2014). Hence, the high methanol emission capacity of juvenile developing leaves (Hüve et al. 2007; Fares et al. 2010) may be limited by the rate of cell division and cell wall expansion rather than by the PME activity.

In contrast to methanol, isoprene emissions showed a strong seasonality, consistent with previous studies (Monson et al. 1994; Kuhn et al. 2004; Wiberley et al. 2005; Niinemets et al. 2010). The onset of isoprene emission was delayed by one month following leaf emergence in the coppiced poplars, similarly to what was observed in a natural poplar stand at high elevation (Monson et al. 1994). In fact, prevailing cold springtime temperatures experienced by the plantation in our study site might have slowed down the expression of the IspS enzyme (Wiberley et al. 2005) in the juvenile developing leaves and, at the same time, might have limited the supply of dimethylallyl diphosphate (DMAPP) substrate for isoprene biosynthesis (Wiberley et al. 2008). The relatively low temperatures throughout most of the growing season constrained the highest isoprene emissions to a very short period in mid-August (Fig. 1g). In addition, the rapid acropetal growth of coppiced poplar shoots occurred along with increasing LAI until the end of August, when LAI reached maximum values and strong isoprene emitting adult leaves outweighed the young ones in all canopy layers (Fig. S1a-d). Therefore, for most of the season, developing poplar leaves from the coppiced plantation released sustained amounts of methanol but were unable to emit isoprene at high rates (Fig. 1b, g). As a whole, juvenile leaves had a higher impact on fluxes of VOC and on GPP than

the adult ones, which became progressively shaded as the canopy closed. The high planting density of bioenergy plantations (Verlinden et al. 2015) further limited light availability for adult poplar leaves in the middle or in the lower layers of the canopy to efficiently photosynthesize and perform light-dependent isoprene biosynthesis.

Overall, the total carbon emitted in the form of isoprene accounted for only 0.7 % of the net ecosystem carbon exchange in the plantation (Tab. 3). This was quite a low percentage when compared to the 1-3 % of the photosynthetically assimilated carbon normally released by poplars as isoprene during a season (Goldstein et al. 1998), which can also increase to 15-50% for short periods in poplar leaves exposed to extreme conditions in the Mediterranean area (Brilli et al. 2007), or - at ecosystem level - in tropical (Harley et al. 2004) and temperate forests (Seco et al. 2015). Isoprene emissions may in the short term be uncoupled from GPP either under stressed (Brilli et al. 2007) or normal conditions (Brilli et al. 2014). However, isoprene emission and photosynthesis are intimately linked as both are light- and temperature-dependent for energy requirements and because photosynthesis supplies the carbon to the Methyl Erythritol Phosphate (MEP-) pathway (Loreto & Sharkey, 1993; Delwiche & Sharkey, 1993). In fact, a strong relationship between isoprene emissions and GPP was found in deciduous tropical trees (Kuhn et al. 2004). Despite isoprene emission being delayed with respect to the beginning of the growing season, we thus confirm that canopy scale photosynthesis may be a reliable basis to model the seasonal variation of isoprene emissions (Niinemets et al. 1999; Grote et al. 2014). Indeed, the seasonal trend of isoprene emission followed the GPP trend, simultaneously reaching their maximum rates (Fig. 4a, b).

Real-time full detection of VOC by PTR-TOF-MS demonstrated the bidirectional exchange of many VOC above the plantation, other than isoprene and methanol (Niinemets et al. 2014).

This was consistent with one previous study at ecosystem level (Park et al. 2013). The SOM visualization revealed that emissions of acetaldehyde, acetone, formic acid, ethanol and a fragment of GLVs were all enhanced under low values of GPP and LAI (Fig. 2c, d, e, f, k, p, t), being associated to the breakdown of cell membranes in senescent leaves after summer (Karl et al. 2005; Brilli et al. 2012). In addition, secondary oxidation products of isoprene (i_{ox}) (Liu et al., 2012) and MEK (McKinney et al. 2011) were emitted when high Tair coupled with high PAR (Fig. 2h, i, q, r) favored photochemical reactions either in the lower atmosphere or within the leaves (Jardine et al. 2012). Due to the short lag-time between the diurnal peak of isoprene emissions at noon and that of i_{ox} a few hours later (Brilli et al. 2014), we cannot exclude that part of the signal recorded at m/z = 71.049 was related to the dominant first-generation isoprene oxidation products (ISOPOOHs) overlapping with MVK and MAC. Indeed, recent findings (Rivera-Rios et al. 2014) support the idea that the production and the release of ISOPOOHs could have preceded the formation of i_{ox} as fast isoprene oxidation already occurs within the leaf mesophyll (Jardine et al. 2012; Fares et al. 2015).

Our results confirmed that poplars remove oxygenated VOC from the atmosphere (Karl et al. 2010). However, if oxygenated VOC do not undergo rapid metabolic transformation into other chemical species after deposition (Oikawa & Lerdau, 2013), they could possibly be re-emitted rapidly - because of their high volatility (Niinemets et al. 2004) - through the evaporation of liquid pools either inside- or outside- the leaves mesophyll where they concentrate. The plantation was a net sink only for formaldehyde (Tab. 3; Brilli et al. 2014). The SOM showed that high rates of formaldehyde deposition were related in the long term to both environmental (i.e. high Tair, PAR, VPD; Fig. 2a, q, r, s) and physiological (high ET rates; Fig. 2a, n) factors determining stomatal opening. This is consistent with previous results at leaf level showing the uptake of formaldehyde to be partially dependent on stomatal

conductance in Mediterranean plant species (Seco et al. 2008). Moreover, the slow and steady deposition of formaldehyde during the season (Fig. 4b) suggested efficient detoxification of formaldehyde in poplar leaves by enzymatic oxidation (Giese et al. 1994).

Uncertainties of MEGAN model parameterization (Guenther et al. 2012) are mainly caused by the short- and long-term seasonal and developmental variation of BEF (Niinemets et al. 2010). We show that the prediction accuracy of the seasonality of both methanol and isoprene emissions could be increased through accurate modeling of BEF by using a function to account for the changes in the enzymatic capacity to produce VOC, as previously observed in the case of isoprene (Schnitzler et al. 1996). Therefore, a function similar to that adopted by Kemper-Pacheco et al. (2014) was generated in this study on the basis of the seasonal trend of two physiological factors potentially responsible for the variable BEF performances such as GPP and LAI. Indeed, our study showed that in the fast-growing 'coppiced' bioenergy poplar plantations, the rapid development of LAI and GPP paralleled the amount of carbon emitted (Fig. 4), and particularly of isoprene and methanol emission capacity over the season. Besides, the maximum capacity of the poplar plantation to form isoprene corresponds to the maximum GPP (Kuhn et al. 2004), LAI might be much more linked to intrinsic leaf properties (and thus to BEF) than GPP, which represents the gross carbon photosynthetically assimilated by the ecosystem, including roots and woody stems in addition to leaves.

As further demonstrated by the lowest AIC values achieved (Tab. 4), MEGAN simulated emissions of methanol and isoprene with more accuracy when BEF was modified to account for the seasonal changes of LAI and GPP. This might be particularly valuable when applied to 'coppiced' isoprene emitting plantations where fast development of a canopy (and thus of LAI) is associated with high GPP rates and methanol emissions. Nevertheless, methanol emission was overestimated during episodes of rapid temperature increase that occurred at

the end of July and in mid-August. Control of methanol emission may depend not only from the variable performances of the PME enzyme. This has been previously supported by the successful application of a purely physical model where the seasonality in the BEF performances was not considered to simulate methanol emissions in the long term (Laffineur et al. 2011). Therefore, simulating the seasonal exchange of methanol by applying the latest MEGAN modeling approach is still inappropriate, due to the current limited understanding of methanol production (and emission). Methanol emission may not obey traditional empirical emission algorithms (i.e. light and temperature dependencies) adopted by MEGAN model, but rather exhibits a bidirectional flux whose physiological drivers (i.e. the rate of cell division or cell expansion; Nemecek-Marshall et al. 1995) are yet to be studied.

Unlike methanol, simulated isoprene emission was higher than the observed one only during the high temperature spell at the end of July. This might suggests that MEGAN is not accurate enough to simulate the isoprene dependency to changing temperatures, which may have led either to an overestimation of emissions at high temperatures or to an underestimation at low temperatures, due to a different sensitivity of IspS to temperature fluctuations occurring during the growing season (Hanson & Sharkey, 2001; Cinege et al. 2009). However, a high temperature-dependence of IspS (resulting in a value of $Q_{10} = e^{10 \times 0.23}$) was previously assessed for our plantation (Brilli et al. 2014) with respect to an investigation in a boreal aspen forest (Fuentes et al. 1999). This might indicate that in a coppiced poplar plantation isoprene emission is mainly limited by IspS expression and amount (Mayrhofer et al. 2005) rather than by IspS activity. Moreover, it is unlikely that isoprene emission was limited by DMAPP supply, as the metabolic flux through the MEP pathway has been never constrained by the photosynthetic carbon assimilation over the season.

In conclusion, this report shows abundant methanol, but smaller than expected isoprene emissions from a high-density 'coppiced' poplar plantation regrown from stools in a temperate region under low summer temperatures and unlimited water supply. The results of our measurements might improve global modelling for prediction of overall VOC fluxes based on a mechanistic (semi-empirical) approach, showing that corrections of BEF are required to account for the variation of VOC-specific physiological and physico-chemical constraints occurring during the growing season.

ACKNOWLEDGMENTS

This study was financially supported by the European Commission's Seventh Framework Programme (FP7/2007-2013) as a European Research Council Advanced Grant (no. 233366, POPFULL) as well as by the Flemish Hercules Foundation as Infrastructure contract ZW09-06. We gratefully acknowledge Joris Cools, Alessandro Zaldei and Eugen Hartungen for assistance during the field campaign, for help with the set-up of the installation, maintenance of the instrument.

REFERENCES

Asensio D., Peñuelas J., Filella I., Llusià J. (2007) On-line screening of soil VOCs exchange responses to moisture, temperature and root presence. *Plant Soil* 291, 249-261.

Ashworth K., Folberth G., Hewitt C.N., Eild O. (2012) Impacts of near-future cultivation of biofuel feedstocks on atmospheric composition and local air quality. *Atmospheric Chemistry and Physics* 12, 919-939.

Ashworth K., Wild O., Hewitt C.N. (2013) Impacts of biofuel cultivation on mortality and crop yields. *Nature Climate Change* 3, 492-496.

Bamberger I., Hörtnagl L., Walser M., Hansel A., Wohlfahrt G. (2014) Gap-filling strategies for annual VOC flux data sets, *Biogeosciences* 11, 2429–2442.

Beltman J.B., Hendriks C., Tum M., Schaap M. (2013) The impact of biomass production on ozone air pollution in Europe. *Atmospheric Environment* 71, 352-363.

Brilli F., Barta C., Fortunati A., Lerdau M., Loreto F., Centritto M. (2007) Response of isoprene emission and carbon metabolism to drought in white poplar (*Populus alba*) saplings. *New Phytologist* 175, 244-254.

Brilli F., Ciccioli P., Frattoni hM., Prestininzi M., Spanedda A.F., Loreto F. (2009) Constitutive and herbivore-induced monoterpenes emitted by *Populus* × *euroamericana* leaves are key volatiles that orient *Chrysomela populi* beetles. *Plant Cell & Environment* 32, 542–552.

Brilli F., Hörtnagl L., Bamberger I., Schnitzhofer R., Ruuskanen T.M., Hansel A. (2012) Qualitative and quantitative characterization of volatile organic compound emissions from cut grass. *Environmental Science & Technology* 46, 3859-3865.

Brilli F., Gioli B., Zona D., Pallozzi E., Zenone T., Fratini G., …, Ceulemans R. (2014) Simultaneous leaf- and ecosystem-level fluxes of volatile organic compounds from a poplar-based SRC plantation. *Agricultural and Forest Meteorology* 187, 22–35.

Broeckx L.S., Vanbeveren S.P.P., Verlinden M.S., Ceulemans R. (2015) First *vs* second rotation of a poplar short rotation coppice: leaf area development, light interception and radiation use efficiency. *iForest*, doi: 10.3832/ifor1457-008.

Broeckx L.S., Verlinden M.S., Ceulemans R. (2012) Establishment and two-year growth of a bio-energy plantation with fast-growing Populus trees in Flanders (Belgium): Effects of genotype and former land use. *Biomass and Bioenergy* 42, 151-163.

Brüggeman N., Schnitzler J.P. (2002) Diurnal variation of dimethylallyl diphosphate concentrations in oak (*Quercus robur*) leaves. *Physiologia Plantarum* 115, 190-196.

Cai T.B., Price D.T., Orchansky A.L., Thomas B.R. (2011) Carbon, water, and energy exchanges of a hybrid poplar plantation during the first five years following planting. *Ecosystems* 14, 658-671.

Calfapietra C., Gielen B., Karnosky D., Ceulemans R., Scarascia Mugnozza G. (2010) Response and potential of agroforestry crops under global change. *Environmental Pollution* 158, 1095-1104.

Carlton A.G., Wiedinmyer C., Kroll J.H. (2009) A review of Secondary Organic Aerosol (SOA) formation from isoprene. *Atmospheric Chemistry and Physics* 9, 4987–5005.

Chameides W.L., Lindsay R.W., Richardson J., Kiang C.S. (1988) The role of biogenic hydrocarbons in urban photochemical smog: Atlanta as a case study. *Science* 241, 1473-1475.

Cinege G., Louis S., Hänsch R., Schnitzler J.P. (2009) Regulation of isoprene synthase promoter by environmental and internal factors. *Plant Molecular Biology* 69, 593-604.

Claeys M., Graham B., Vas G., Wang W., Vermeylen R., Pashynska V., …, Maenhaut W. (2004) Formation of secondary organic aerosol through photooxidation of isoprene. *Science* 303, 1173-1176.

Collins W.D., Rasch P.J., Eaton B.E., Fillmore D.W., Kiehl T.J., Beck C.T, Zender C. (2002) Simulation of aerosol distributions and radiative forcing for INDOEX: Regional climate impacts. *Journal of Geophysical Research – Atmosphere* 107, 27-1 – 27-20.

Delwiche C.F., Sharkey T.D. (1993) Rapid appearance of ^{13}C in biogenic isoprene when $^{13}CO_2$ is fed to intact leaves. *Plant Cell & Environment* 16, 587–591.

Dillen S.Y., Vanbeveren S., Alafas N., Laureysens I., Croes S., Ceulemans R. (2011) Biomass production in a 15-years-old short-rotation coppice culture in Belgium. *Aspects of Applied Biology* 112, 99-106.

Ditomaso J.M., Reaser J.K., Dionigi C.P., Doering O.C:, Chilton E., Schardt J.D:, Barney J.N. (2010) Biofuel vs Bioinvasion: Seeding poly priorities. *Environmental Science & Technology* 44, 6906-6910.

Energy Information Administration (2013). *Annual Energy Outlook 2013: Early Release Overview*. In US Energy Information Administration, Washington, DC.

Fall R., Benson A.A. (1996) Leaf methanol – the simplest natural product from plants. Trends in Plant *Science* 1, 296–301.

Fares S., Oksanen E., Lännenpää M., Julkunen-Titto R., Loreto F. (2010) Volatile emissions and phenolic compound concentrations along a vertical profile of *Populus nigra* leaves exposed to realistic ozone concentrations. *Photosynthesis Research* 104, 61–74.

Fares S., Park J.H., Gentner D.R., Weber R., Ormeño E., Karlik J., Goldstein A.H. (2012) Seasonal cycles of biogenic volatile organic compound fluxes and concentrations in a California citrus orchard. *Atmospheric Chemistry and Physics Discussion* 12, 9865-9880.

Fares S., Schnitzhofer R., Jiang X., Guenther A., Hansel A,, Loreto F. (2013) Observations of diurnal to weekly variations of monoterpene-dominated fluxes of Volatile Organic Compounds from Mediterranean forests: implications for regional modeling. *Environmental Science & Technology* 19, 11073-11082.

Fares S., Paoletti E., Loreto F., Brilli F. (2015) Bidirectional flux of methyl vinyl ketone and methacrolein in trees with different isoprenoids emission under realistic ambient concentrations. *Environmental Science Technology* 49, 7735-7742.

Fratini G., Ibrom A., Arriga N., Burba G., Papale D. (2012) Relative humidity effects on water vapour fluxes measured with closed-path eddy-covariance systems with short sampling lines. *Agricultural and Forest Meteorology* 147, 209–232.

Fuentes J.D., Wang D., Gu L. (1999) Seasonal variations in isoprene emissions from a boreal aspen forest. *Journal of Applied Meteorology* 38, 855-869.

Gaffe J., Tuieman D.M., Handa A.K. (1994) Pectin methylesterase isoforms in tomato (*Lycopersicon esculentum*) tissues. Effects of expression of a pectin methylesterase antisense gene. *Plant Physiology* 105, 199-203.

Galbally I.E., Kristine W. (2002) The production of methanol by flowering plants and the global cycle of methanol. *Journal of Atmospheric Chemistry* 43, 195-229.

Gelfand I., Zenone T., Jasrotia P., Chen J., Hamilton S.K., Robertson G.P. (2011) carbon debt of conservation reserve program (CRP) grassland converted to bioenergy production. *Proceedings of the National Academy of Sciences* 108, 13864-13869.

Giese M., Bauer-Doranth U., Langebartels C., Sandermann H.J. (1994) Detoxification of Formaldehyde by the Spider Plant (*Chlorophytum comosum* L.) and by Soybean (*Glycine max* L.) Cell-Suspension Cultures. *Plant Physiology* 104, 1301-1309.

Göckede M., Rebmann C., Folken T. (2004) A combination of quality assessment tools for eddy covariance measurements with footprint modelling for the characterization of complex sites. *Agricultural and Forest Meteorology* 127, 175-188.

Goldstein A.H., Goulden M.L., Munger W., Wofsy S.C., Geron C. (1998) Seasonal course of isoprene emissions from a midlatitude deciduous forest. *Journal of Geophysical Research* 103, 31045-31056.

Gout E., Aubert S., Bligny R. (2000) Metabolism of methanol in plant cells. Carbon-13 nuclear magnetic resonance studies. *Plant Physiology* 123, 287–296

Graus M., Müller M., Hansel A. (2010) High resolution PTR-TOF quantification and formula confirmation of VOC in real time. *Journal American Society Mass Spectrometry* 21, 1037-1044.

Grote R., Morfopoulos C., Niinemets U., Zhihong S., Keenan T.F., Pacifico F., Butler T. (2014) A fully integrated isoprenoid emissions model coupling emissions to photosynthetic characteristics. *Plant Cell & Environment* 37, 1965–1980.

Guidolotti G., Calfapietra C., Loreto F. (2011) The relationship between isoprene emission, CO*2* assimilation and water use efficiency across a range of poplar genotypes. *Physiologia Plantarum* 142, 297-304.

Guenther A., Hewitt C.N., Erickson D., Fall R., Geron C., Graedel T., …, Zimmerman P. (1995) A global model of natural volatile organic compound emissions. *Journal Geophysical Research* 100, 8873–8892.

Hakola H., Rinne J., Laurilla T. (1998) The hydrocarbon emission rates of tea-leafed willow (*Salix phylicifolia*), silver birch (*Betula pendula*) and European Aspen (*Populus tremula*). *Atmospheric Environment* 33, 1821-1833.

Guenther A., Jiang X., Heald C.L., Sakulyanontvittaya T., Duhl T., Emmons L.K., Wang X. (2012) The Model of Emissions of Gases and Aerosols from Nature version 2.1 (MEGAN2.1): an extended and updated framework for modeling biogenic emissions. *Geoscientific Model Development* 5, 1471–1492.

Hakola A., Rinne J., Laurila T. (1998) The hydrocarbon emission rates of tea-leafed willow (*Salix phylicifolia*), silver birch (*Betula pendula*) and European aspen (*Populus tremula*). *Atmospheric Environment* 10, 1825-1833.

Hanson D.T., Sharkey T.D. (2001) Rate of acclimation of the capacity for isoprene emission in response to light and temperature. *Plant Cell & Environment* 24, 937–946.

Harley P, Vasconcellos P., Vierling L., Cleomir De S. Pinheiros C., Greenberg J., …, Malhi Y. (2004) Variation in potential for isoprene emissions among neotropical forest sites. *Global Change Biology* 10, 630-650.

Holzinger R., Kasper-Giebl A., Staudinger M., Schauer G., Röckmann T. (2010) Analysis of the chemical composition of organic aerosol at the Mt. Sonnblick observatory using a novel high mass resolution thermal-desorption proton-transfer-reaction mass-spectrometer (hr-TD-PTR-MS). *br* 10, 10111-10128.

Hüve K., Christ M.M., Kleist E., Uerlings R., Niinemets U., Walter A., Wildt J. (2007) Simultaneous growth and emission measurements demonstrate an interactive control of methanol release by leaf expansion and stomata. *Journal Experimental Botany* 58, 1783-1793.

IPCC. *The IPCC special report on renewable energy sources and climate change mitigation* (2011). O. Edenhofer, R. Pich-Madruga, Y. Sokona , K. Seyboth. Eds Cambridge University Press.

Jacob D.J., Field B.D., Li D. (2005) Global budget of methanol: constraints from atmospheric observations. *Journal of Geophysical Research-Atmosphere* 110, doi:10.1029/2004JD005172.

Jardine K.J., Monson R.K., Abrell L., Saleska S.R., Arneth A., Jardine A., …, Huxman T. (2012) Within-plant isoprene oxidation confirmed by direct emissions of oxidation products methyl vinyl ketone and methacrolein. *Global Change Biology* 18, 973-984.

Jordan A., Haidacher S., Hanel G., Hartungen E., Märk L., Seehauser H., …, Märk T.D. (2009) A high resolution and high sensitivity proton-transfer-reaction time-of-flight mass spectrometer (PTR-TOF-MS). *International Journal of Mass Spectrometry* 286, 122-128.

Karl T., Potosnak M., Guenther A., Clark D., Walker J., Herrick J.D., Geron C. (2004) Exchange processes of volatile organic compounds above a tgrropical rain forest: Implications for modeling tropospheric chemistry above dense vegetation. *Journal of Geophysical Research-Atmosphere* 109, DOI: 10.1029/2004JD004738.

Karl T., Harren F., Warneke C., de Gouw J., Grayless C., Fall R. (2005) Senescing grass crops as regional sources of reactive volatile organic compounds. *Journal of Geophysical Research-Atmosphere* 110, D15302, doi:10.1029/2005JD005777 .

Karl T., Guenther A., Turnipseed A., Patton E.G., Jardine K. (2008) Chemical sensing of plant stress at ecosystem scale. *Biogeosciences* 5, 1287-1294.

Karl T., Harley P., Emmons L., Thornton B., Guenther A., Basu C., …, Jardine K. (2010) Efficient atmospheric cleansing of oxidized organic trace gases by vegetation. *Science* 330, 816–819.

Kemper-Pacheco C., Fares S., Ciccioli P. (2014) A highly spatially resolved GIS-based model to assess the isoprenoid emissions from Italian ecosystems. *Atmospheric Environment* 96, 50-60.

Kesselmeier J., Staudt M. (1999) Biogenic Volatile Organic Compounds (VOC): an overview on emission, physiology and ecology. *Journal of Atmospheric Chemistry* 33, 23-88.

King J.S., Ceulemans R., Albaugh J.M., Dillen S.Y., Domec J.C., Fichot R., …, Zenone T. (2013) The challenge of ligno-cellulosic bioenergy in a water-limited world. *BioScience* 63, 102-117.

Kiviluoto K. (1996) Topology preservation in self-organizing maps. In *Proceedings of the International Conference on Neural Networks* (eds CINN), pp. 294–299. Piscataway, New Jersey.

Koh L., Levang P., Ghazoul J. (2009) Designer landscapes for sustainable biofuels. *Trends Ecology Evolution* 24, 381-384.

Kohonen T. (2001) In *Self-Organizing Maps*, pp. 1-320, Springer, Berlin, Germany.

Kuhn U., Rottenberger S., Biesenthal A., Wolf A., Schebeske G., Ciccioli P., Kesselmeier J. (2004) Strong correlation between isoprene emission and gross photosynthetic capacity during leaf phenology of the tropical tree species *Hymenaea courbaril* with fundamental changes in volatile organic compounds emission composition during early leaf development. *Plant Cell & Environment* 27, 1469-1485.

Laffineur Q., Aubinet M., Schoon N., Amelynck C., Müller J.F., Dewulf J., …, Heinesch B. (2011) Abiotic and biotic control of methanol exchanges in a temperate mixed forest. *Atmospheric Chemistry Physics* 12, 577-590.

Langford B., Misztal P.K., Nemitz E., Davison B., Helfter C., Pugh T.A.M., …Hewitt C.N. (2010) Fluxes and concentrations of volatile organic compounds from a South-East Asian tropical rainforest. *Atmospheric Chemistry Physics* 10, 8391-8412.

Laothawornkitkul J., Paul N.D., Vickers C.E., Possell M., Taylor J.E., Mullineaux P.M., Hewitt N. (2008) Isoprene emissions influence herbivore feeding decisions. *Plant Cell and Environment* 31, 1410-1415.

Liu Y.J., Herdlinger-Blatt I., McKinney K.A., Martin S.T. (2012) Production of methyl vinyl ketone and methacrolein via the hydroperoxyl pathway of isoprene oxidation. *Atmospheric Chemistry and Physics* 13, 5715-5730.

Lloyd J., Taylor J.A. (1994) On the temperature dependence of soil respiration. *Functional Ecology* 8, 315–323.

Loivamaäki M., Mumm R., Dicke M., Schnitzler J.P. (2010) Isoprene interferes with the attraction of bodyguards by herbaceous plants. *Proceedings of the National Academy of Sciences* 105, 17430-17435.

Loreto F., Sharkey T.D. (1990) A gas-exchange study of photosynthesis and isoprene emission in *Quercus rubra* L. *Planta* 182, 523-531.

Loreto F., Sharkey T.D. (1993) On the relationship between isoprene emission and photosynthetic metabolites under different environmental conditions. *Oecologia* 189, 420-424.d

Loreto F., Barta C., Brilli F., Nogues I. (2006) On the induction of volatile organic compound emissions by plants as consequence of wounding or fluctuations of light and temperature. *Plant Cell & Environment* 29, 1820–1828.

Loreto F., Schnitzler J.P. (2010) Abiotic stresses and induced BVOCs. *Trends in Plant Sciences* 15, 154-166.

Loreto F., Dicke M., Schnitzler J.P., Turling T.C.J. (2014) Plant volatiles and the environment. *Plant Cell & Environment* 37, 1905-1908.

Loreto F., Fineschi S. (2015) Reconciling functions and evolution of isoprene emission in higher plants. *New Phytologist* 206, 578-582.

Luyssaert S., Janssens A.J., Sulkava M., Papale D., Dolman A.J., Reichstein M. (2007) Photosynthesis drives anomalies in net carbon-exchange of pine forests at different latitudes. *Global Change Biology* 13, 2110-2127.

McKinney K.A., Lee B.H., Vasta A., Pho T.V., Mungen J.W. (2011) Emissions of isoprenoids and oxygenated biogenic volatile organic compounds from a New England mixed forest. *Atmospheric Chemistry and Physics* 11, 4807-4831.

Migliavacca M., Meroni M., Manca G., Matteucci G., Montagnani L., Grassi G., …, Seufert G. (2009) Seasonal and interannual patterns of carbon and water fluxes of a poplar plantation under peculiar eco-climatic conditions. *Agricultural and Forest Meteorology* 147, 209-232.

Mayrhofer S., Teuber M., Zimmer I., Luois S., Fischbach R.J., Schnitzler J.P. (2005) Diurnal and seasonal variation of isoprene biosynthesis-related genes in grey poplar leaves. *Plant Physiology* 139, 474-484.

Miresmailli S., Zeri M., Zangerl A.R:, BErnacchi C.J., Berenbaum M.R., DeLucia E.H. (2013) Impact of herbaceous bioenergy crop on atmospheric volatile organic composition and potential consequences for global climate change. *Bioenergy* 5, 375-383.

Misztal P.K., Nemitz E., Langford B., Di Marco C.F., Phillips G.J., Hewitt C.N., …Cape N.J. (2011) Direct ecosystem fluxes of volatile organic compounds from oil palms in South-East Asia. *Atmospheric Chemistry and Physics* 11, 8995-9017.

Moffat A.M., Papale D., Reichstein M., Hollinger D.Y., Richardson A.D., Barr A.G., …, Stauch V.J. (2007) Comprehensive comparison of gap-filling techniques for eddy covariance net carbon fluxes. *Agricultural and Forest Meteorology* 147, 209-232.

Monson R.K., Harley P.C., Litvak M.E., Wildermuth M., Guenther A.B., Zimmermann P.R., Fall R, (1994) Environmental and developmental control over the seasonal pattern of isoprene emission from aspen leaves. *Oecologia* 99, 260-270.

Müller M., Mikoviny T., Jud W., D'Anna B., Wisthaler A. (2013) A new software tool for the analysis of high resolution PTR-TOF mass spectra. *Chemometrics and Intelligent Laboratory Systems* 127, 158-165.

Nemecek-Marshall M., Macdonald R.C., Franzen F.J., Wojciechowski C.L., Fall R. (1995) Methanol emission from leaves – enzymatic detection of gas-phase methanol and relation of methanol fluxes to stomatal conductance and leaf development. *Plant Physiology* 108, 1359-1368.l

Niinemets U., Tenhunen J.D., Harley P.C., Steinbrecher R. (1999) A model of isoprene emission based on energetic requirements for isoprene synthesis and leaf photosynthetic properties in *Liquidambar* and *Quercus*. *Plant Cell & Environment* 22, 1319-1335.

Niinemets Ü., Reichstein M. (2003) Controls on the emission of plant volatiles through stomata: differential sensitivity of emission rates to stomatal closure explained. *Journal of Geophysical Research* 108, 4208.

Niinemets U., Loreto F., Reichstein M. (2004) Physiological and physicochemical controls on foliar volatile organic compound emissions. *Trends in Plant Science* 9, 180-186.

Niinemets U., Arneth A., Kuhn U., Monson R.K., Peñuelas J., Staudt M. (2010) The emission factor of volatile isoprenoids: stress, acclimation, and developmental responses. *Biogeosciences* 7, 2203-2223.

Niinemets U., Fares S., Harley P., Kolby J.J. (2014) Bidirectional exchange of biogenic volatiles with vegetation: emission sources, reactions, breakdown and deposition. *Plant Cell & Environment* 37, 1790-1809.

Oikawa P.Y., Giebel B.M., Sternberg L., Li L., Timko M.P., Swart P.K., …, Lerdau M.T. (2011a) Leaf and root pectin methylesterase activity and C-13/C-12 stable isotopic ratio measurements of methanol emissions give insight into methanol production in *Lycopersicon esculentum*. *New Phytologist* 191, 1031-1040.

Oikawa P.Y., Li L., Timko M.P., Mak J.E., Lerdau M.T. (2011b) Short term changes in methanol emission and pectin methylesterase activity are not directly affected by light in *Lycopersicon esculentum*. *Biogeosciences* 8, 1023-1030.

Oikawa P.Y., Lerdau M.T. (2013) Catabolism of volatile organic compounds influences plant survival. *Trends in Plant Science* 18, 695-703.

Oja M., Kaski S., Kohonen T. (2003) Bibliography of self-organizing map (SOM) papers: 1998–2001 addendum. *Neural Computing Surveys* 3, 1-156.

Ou X.M., Zhang X.L., Chang S.Y., Guo Q.F. (2009) Energy consumption and GHG emissions of six biofuel pathways by LCA in (the) People's Republic of Cina. *Applied Energy* 86, S197-S208.

Özdemir E.D., Härdtlein M., Eltrop L. (2009) Land substitution effects of biofuel side products and implications on the land area requirement for EU 2020 biofuel targets. *Energy Policy* 37, 2986-2996.

Palmer P.I., Jacob D.J., Fiore A.M., Martin R.V., Chance K., Kurosu, T.P. (2003) Mapping isoprene emissions over North America using formaldehyde column observations from space. *Journal of Geophysical Research-Atmosphere* 108, doi:10.1029/2002JD002153 .

Papale D., Reichstein M., Aubinet M., Canfora E., Bernhofer C., Kutsch W., ..., Longdoz B. (2006) Towards a standardized processing of Net Ecosystem Exchange measured with eddy covariance technique: algorithms and uncertainty estimation, Biogeosciences 3, 571-583.

Park J.H., Goldstein A.H., Timkovsky J., Fares S., Weber R., Karlik J., Holzinger R. (2013) Active atmosphere-ecosystem exchange of the vast majority of detected volatile organic compounds. *Science* 341, 643-647.

Penuelas J., Asensio D., Tholl D., Wenke K., Rosenkranz M., Piechulla B., Schnitzler J.P. (2014) Biogenic volatile emissions from the soil. *Plant Cell & Environment* 37, 1866-1891.

Pita G, .Gielen B., Zona D., Rodrigues A., Rambal S., Janssens I.A., Ceulemans R. (2013) Carbon and water vapor fluxes over four forests in two contrasting climatic zones. *Agricultural and Forest Meteorology* 180, 211-224.

Porter W.C., Rosenstiel T.N., Guenther A., Lamarque J-F., Bersanti K. (2015) Reducing the negative human-health impacts of bioenergy crop emissions through region-specific crop selection. *Environmental Research Letters* 10, 050404.

Porter W.C., Bersanti K.C., Baughman E.C., Rosenstiel T.N. (2012) Considering the air quality impact of bioenergy crop production: a case study involving *Arundo donax*. *Environmental Science Technology* 46, 9777-9784.

Rasulov B., Bischele I., Laisk A., Niinemets U. (2014) Competition between isoprene emission and pigment synthesis during leaf development in aspen. *Plant Cell & Environment* 37, 724-741.

Rasulov B., Bischele I., Hüve K., Vislap V., Niinemets U. (2015) Acclimation of isoprene emission and photosynthesis to growth temperature in hybrid aspen: resolving structural and physiological controls. *Plant Cell & Environment* 38, 751-766.

Reichstein M., Falge E., Baldocchi D. (2005) On the separation of net ecosystem exchange into assimilation and ecosystem respiration: Review and improved algorithm. *Global Change Biology* 11, 1424-1439.

Rivera-Rios J.C., Nguyen T.B., Crounse J.D., Jud W., St. Clair J.M., Mikoviny T., …, Keutsch F.N. (2014) Conversion of hydroperoxides to carbonyls in field and laboratory instrumentation: observational bias in diagnosing pristine versus anthropogenically-controlled atmospheric chemistry. *Geophysical Research Letter* 41, 8645-8651.

Schnitzler J.P., Lehning A., Steinbrecher R. (1996) Seasonal pattern of isoprene synthase activity in Quercus robur leaves and its significance for modelling isoprene emission rates. *Botanica Acta* 110, 240-243.

Searchinger T., Heimlich R., Houghton R.A., Dong F.X., Elobeid A., Fabiosa J.,…, Yu T.D. (2008) Use if US croplands for biofuels increases greenhouse gasses through emissions from land-use change. *Science* 319, 1238-1240.

Seco R., Peñuelas J., Filella J. (2008) Formaldehyde emission and uptake by Mediterranean trees *Quercus ilex* and *Pinus alepensis*. *Atmospheric Environment* 42, 7907-7914.

Seco R., Karl T., Guenther A., Hosman K.P., Pallardy S.G., Lianhoung G., …, Seawung K. (2015) Ecosystem-scale volatile organic compound fluxes during an extreme drought in broadleaf temperate forest of the Missouri Ozarks (central USA). *Global Change Biology* DOI: 10.1111/gcb.12980

Shade G.W., Solomon S.J., Dellwik E., Pilegaard K., Ladstätter-Weissenmayer A. (2011) Methanol and other VOC fluxes from a Danish beech forest during late springtime. *Biogeochemistry* 106, 337-355.

Shallcross D.E., Monks P.S. (2000). New Directions: A role for isoprene in biosphere-climate chemistry feedbacks. *Atmospheric Environment* 34, 1659-1660.

Sinderalova K., Granier C., Bouarar I., Guenther A., Tilmes S., Stavrakou T., …, Knorr W. (2014) Global data set of biogenic VOC emissions calculated by the MEGAN model over the last 30 years. *Atmospheric Chemistry and Physics* 14, 9317-9341.

Tie X., Guenther A., Holland E. (2003) Biogenic methanol and its impacts on tropospheric oxidants. *Geophysical Research Letters* 30, doi:10.1029/2003GL017167.

Van Poecke R.M.P., Posthumus M.A., Dicke M. (2001) Herbivore-induced volatile production by *Arabidopsis thaliana* leads to attraction of the parasitoid *Cotesia rubecula*: Chemical, behavioral, and gene-expression analysis. *Journal of Chemical Ecology* 27, 1911-1928.

Verlinden M.S., Broeckx L.S., Ceulemans C. (2015) First vs. second rotation of a poplar short rotation coppice: Above-ground biomass productivity and shoot dynamics. *Biomass and Bioenergy* 73, 174-185.

Vickers C.E., Gershenzon J., Lerdau M.T., Loreto F. (2009) A unified mechanism of action for volatile isoprenoids in plant abiotic stress. *Nature Chemical Ecology* 5, 283–291.

Von Dahl C.C., Hävecker M., Schlögl R., Baldwin I.T. (2006) Caterpillar-elicited methanol emission: a new signal in plant-herbivore interactions? *Plant Journal* 46, 948-960.

Weih M. (2004) Intensive short rotation forestry in boreal climates: present and future perspectives. *Canadian Journal Forest Research* 34, 1369-1378.

Wiberley A.E., Linskey A.R., Falbel T.G., Sharkey T.D. (2005) Development of the capacity for isoprene emission in kudzu. *Plant Cell & Environment* 28, 898-905.

Wiberley A.E., Donohue A.R., Meier M.E., Westphal M.M., Sharkey T.D. (2008) Regulation of isoprene emission capacity throughout a day. *Plant Cell & Environment* 31, 258-267.

Wohlfahrt G., Amelynck C., Ammann C., Arneth A., Bamberger I., Goldstein A.H. (2015) An ecosystem-scale perspective of the net land methanol flux: synthesis of micrometeorological flux measurements. *Atmospheric Chemistry and Physics Discussion* 15, 2577-2613.

Zenone T., Fischer M., Arriga N., Broeckx L.S., Verlinden M.S., Vanbeveren S., Zona D., Ceulemans R. (2015) Biophysical drivers of the carbon dioxide, water vapor, and energy exchanges of a short-rotation poplar coppice. *Agricultural and Forest Meteorology* 209, 22-35.

Zona D., Janssens I., Gioli B., Jungkunst H.F., Serrano M.C., Ceulemans R. (2012) N_2O fluxes of a bio-energy poplar plantation during a two years rotation period. *Global Change Biology Bioenergy* 5, 536-547.

Zona D., Janssens I., Aubinet M., Gioli B., Vicca S., Ceulemans R. (2013) Fluxes of the greenhouse gases (CO_2, CH_4 and N_2O) above a short-rotation poplar plantation after conversion from agricultural land. Agricultural and Forest Meteorology 169, 100-110.

Table 1. Summary statistics for eddy covariance fluxes (nmol m^{-2} s^{-1}) of volatile organic compounds (VOC) measured during the entire period from 4 June to 31 October 2012. In parenthesis, the statistical values are provided for fluxes that have successfully passed all the quality criteria mentioned in section 2.2 of Materials & Methods. SE = standard error; N = number of data; 95^{th} % ile = 95^{th} percentile; 5^{th} % ile = 5^{th} percentile; Min=minimum value; Max = maximum value.

VOC	Mean	SE	95^{th} % ile	5^{th} % ile	Median	Min	Max	N
Formaldehyde m/z 31.018 (CH_2O-H^+)	-0.015 (-0.016)	0.002 (0.002)	0.291 (0.257)	-0.332 (-0.297)	-0.100 (-0.013)	-0.890 (-0.891)	1.067 (1.067)	5652 (7200)
Methanol m/z 33.033 (CH_4O-H^+)	0.884 (0.924)	0.022 (0.017)	4.171 (3.815)	-0.702 (-0.530)	0.388 (0.497)	-8.694 (-5.826)	18.958 (18.958)	5737 (7200)
Acetaldehyde m/z 45.033 (CH_4O-H^+)	0.004 (0.005)	0.002 (0.002)	0.273 (0.239)	-0.261 (-0.232)	0.002 (0.006)	-0.992 (-0.992)	1.064 (0.838)	5584 (7200)
Formic Acid m/z 47.012 (CH_2O_2-H^+)	0.015 (0.017)	0.004 (0.003)	0.462 (0.384)	-0.378 (-0.312)	0.002 (0.010)	-5.427 (-2.527)	3.102 (3.102)	5681 (7200)
Ethanol m/z 47.070 (C_2H_6O-H^+)	0.004 (0.004)	0.004 (0.003)	0.181 (0.174)	-0.159 (-0.146)	-0.002 (-0.002)	-9.888 (-9.888)	11.073 (4.24)	5810 (7200)
Acetone m/z 59.049 (C_3H_6O-H^+)	0.035 (0.037)	0.004 (0.003)	0.412 (0.347)	-0.312 (-0.255)	0.016 (0.031)	-2.438 (-1.849)	8.474 (8.474)	5682 (7200)
Isoprene m/z 69.069 (C_5H_8-H^+)	1.009 (1.017)	0.037 (0.031)	5.611 (5.202)	-0.216 (-0.188)	0.153 (0.166)	-2.633 (-2.633)	38.661 (38.661)	5803 (7200)
i_{OX} m/z 71.049 (C_4H_6O-H^+)	0.003 (0.004)	0.001 (0.001)	0.098 (0.088)	-0.086 (-0.077)	0.001 (0.002)	-0.247 (-0.247)	0.351 (0.257)	5660 (7200)
MEK m/z 73.068 (C_4H_8O-H^+)	0.004 (0.005)	0.001 (0.001)	0.156 (0.138)	-0.141 (-0.123)	0.001 (0.005)	-0.562 (-0.526)	0.668 (0.668)	5700 (7200)
GLV & monoterpenes fragment m/z 81.069 (C_6H_8-H^+)	0.008 (0.008)	0.001 (0.001)	0.111 (0.098)	-0.089 (-0.078)	0.004 (0.006)	-0.755 (-0.755)	0.613 (0.550)	5709 (7200)
GLV fragment m/z 83.086 (C_3H_{10}-H^+)	0.031 (0.139)	0.009 (0.012)	0.857 (1.632)	-0.730 (-1.191)	0.005 (0.061)	-6.434 (-11.991)	7.550 (23.369)	5686 (7200)
Σ Monoterpenes m/z 137.133 ($C_{10}H_{16}$-H^+)	0.005 (0.003)	0.001 ($4*10^{-4}$)	0.077 (0.059)	-0.063 (-0.048)	0.002 (0.003)	-0.359 (-0.209)	1.354 (0.237)	5782 (7200)

Table 2. Parameters of the best fit for data selected between daytime hours (7:00-20:00) in different months are: R^2, correlation coefficient and *a*, regression slope ± standard error ($p < 0.05$).

		Regression line	R^2		*a*	
			Methanol	Isoprene	Methanol	Isoprene
PAR	*June*	$f = y_0 + a \ln(abs(x))$	0.08	0.22	146±16	155±12
	July		0.18	0.39	187±11	229±12
	August		0.21	0.37	157±11	158±8
	September		0.29	0.57	160±10	199±8
	October		---	0.22	---	146±10
	Temperature *June*		0.07	0.38	7±0.3	11±0.2
	July		0.17	0.48	8±0.3	10±0.2
	August		0.13	0.24	8±0.2	7±0.1
	September		0.14	0.33	7±0.2	8±0.2
	October		0.05	0.10	6±0.3	11±1
VPD *June*		$f = b + ax$	0.07	0.34	0.06	0.12
	July		0.20	0.51	0.15	0.16
	August		0.18	0.37	0.09	0.04
	September		0.17	0.43	0.07	0.11
	October		0.10	0.27	0.06	0.28
GPP *June*		$f = a \ln(abs(x-x_0))$	0.09	0.42	6±0.3	13±0.3
	July		0.16	0.17	10±0.4	9±0.3
	August		0.34	0.42	13±0.3	11±0.2
	September		0.31	0.52	15±0.4	18±0.4
	October		0.02	0.16	4±0.4	12±1
ET *June*		$f = a \ln(abs(x-x_0))$	0.12	0.42	2±0.1	3±0.1
	July		0.27	0.55	2±0.1	3±0.1
	August		0.38	0.70	3±0.1	2±0.1
	September		0.38	0.68	2±0.1	3±0.1
	October		0.06	0.22	1±0.1	2±0.1

Table 3. Cumulative sum of the carbon emitted, deposited and balanced (= emitted-deposited) in the form of the most abundant volatile organic compounds (VOC), total net ecosystem exchange (NEE) of CO_2, gross primary production (GPP), and respiration (RECO) of the poplar plantation during the growth period (4 June to 31 October 2012).

Cumulative Fluxes	**Emission (gC m^{-2})**	**Deposition (gC m^{-2})**	**Balance (gC m^{-2})**
Formaldehyde (*m/z* 31.018)	0.001	- 0.010	-0.099
Methanol (*m/z* 33.033)	0.160	- 0.016	0.144
Acetaldehyde (*m/z* 45.033)	0.027	- 0.022	0.005
Formic acid (*m/z* 47.012)	0.012	- 0.007	0.005
Ethanol (*m/z* 47.050)	0.012	- 0.011	0.001
Acetone (*m/z* 59.049)	0.041	- 0.024	0.017
Isoprene (*m/z* 69.070)	0.815	- 0.024	0.791
i_{ox} (*m/z* 71.049)	0.011	- 0.009	0.002
MEK (*m/z* 73.068)	0.018	- 0.015	0.003
GLV & Monoterpenes fragment (*m/z* 81.070)	0.021	- 0.013	0.007
GLV fragment (*m/z* 83.085)	0.034	- 0.021	0.013
Σ Monoterpenes (*m/z* 137.133)	0.020	- 0.014	0.005
NEE	---	-115.124	---
RECO	1278.254	---	---
GPP	---	---	1393.277

Table 4. Statistics on the gap filled fluxes of methanol and isoprene (nmol m^{-2} s^{-1}) measured from 4 June to 31 October 2012 with respect to the Model of Emissions of Gases and Aerosols from Nature (MEGAN) simulated fluxes (nmol m^{-2} s^{-1}). Either a constant or a dynamic basal emission factor (BEF) was applied, the latter based on the seasonal variation of gross primary production (GPP) and leaf area index (LAI). R^2 is the correlation coefficient ($p < 0.05$), RSME is the root mean squared error and AIC is the Akaike information criterion between the measured and their modeled values.

Fluxes *(nmol m^{-2} s^{-1})*	**Measured (gap-filled)**	**Modeled (with constant BEF)**	**Modeled (with dynamic BEF based on GPP)**	**Modeled (with dynamic BEF based on LAI)**
	Methanol			
Mean	0.90	1.19	0.99	0.92
5th percentile	- 0.67	0	0	0
95th percentile	4.18	6.06	5.44	5.26
Std dev	1.63	2.76	2.59	2.42
R^2	1	0.36	0.32	0.32
RSME	5.84	7.52	6.87	6.61
AIC	---	1220.10	1202.92	1175.05
	Isoprene			
Mean	1.03	1.17	0.98	0.91
5th percentile	- 0.21	0	0	0
95th percentile	5.68	5.99	5.37	5.20
Std dev	2.85	2.72	2.56	2.39
R^2	1	0.72	0.75	0.77
RSME	6.29	7.48	6.83	6.57
AIC	---	1106.68	1060.88	1016.55

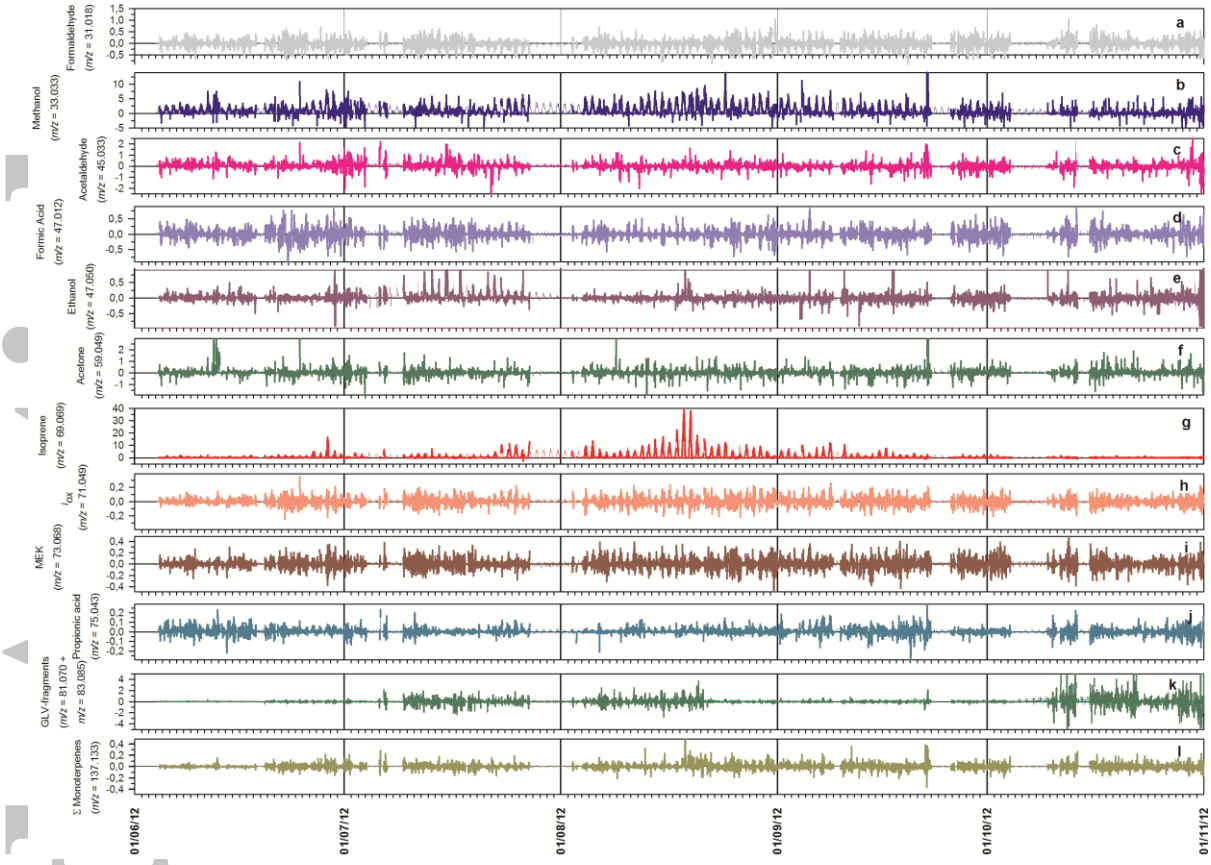

Figure 1. Time series of half-hourly volatile organic compounds (VOC) fluxes (a-l; nmol m^{-2} s^{-1}) measured by PTR-TOF-MS at the field site (thick lines) and gap-filled (hairlines) during the growing season of 4 June – 31 October 2012.

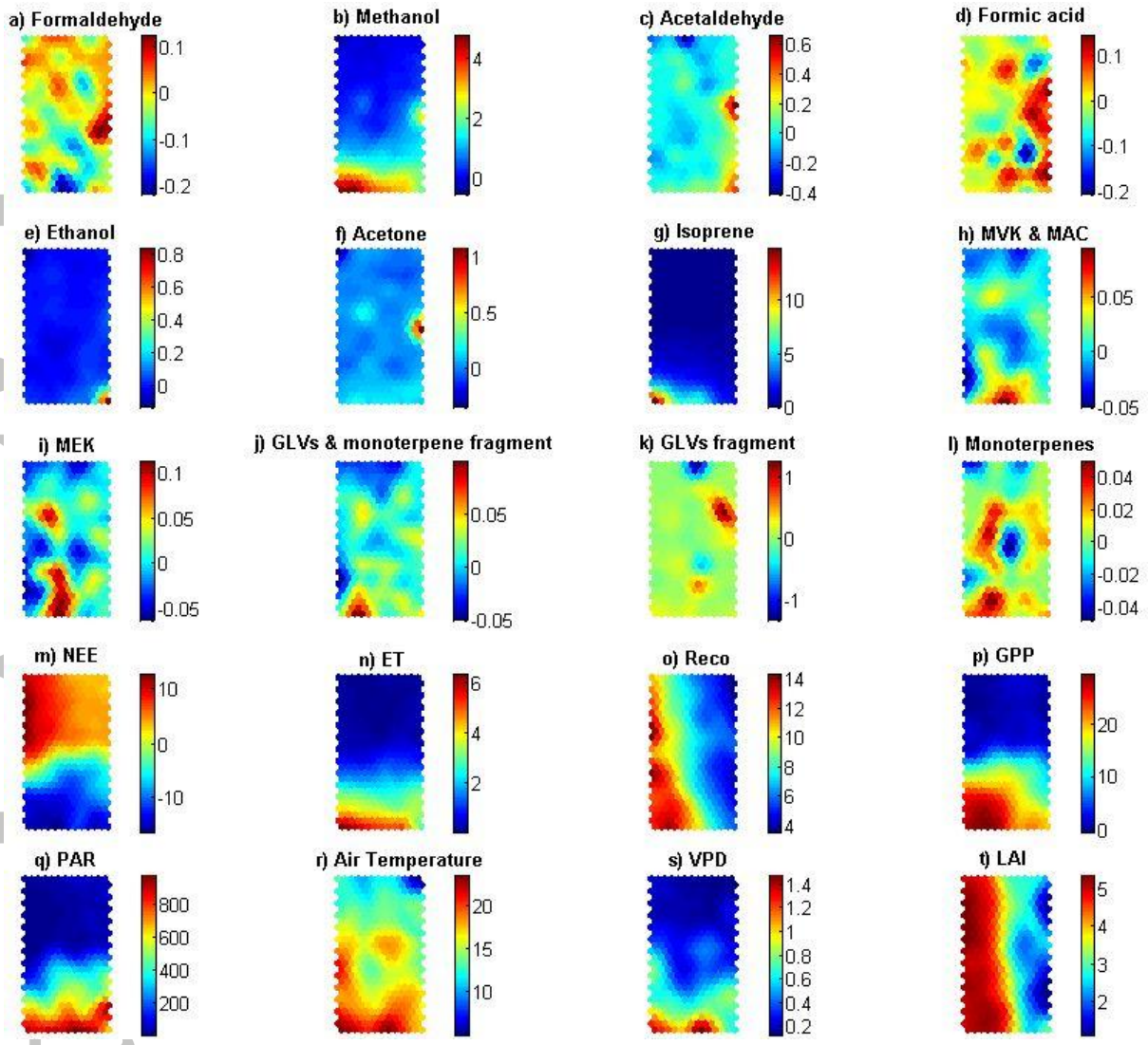

Figure 2. Panels (a-t) are component planes of the Self Organizing Map (SOM) for fluxes of volatile organic compounds (VOC) (a–l; nmol m^{-2} s^{-1}) and the corresponding net ecosystem CO_2 exchange (NEE) (m; µmol m^{-2} s^{-1}), evapotranspiration (ET) (n; mmol m^{-2} s^{-1}), ecosystem respiration (RECO) (o; µmol m^{-2} $s^{-}1$), gross primary production (GPP) (p;µmol m^{-2} s^{-1}), photosynthetic active radiation (PAR) (q; µmol photons m^{-2} s^{-1}), air temperature (r; °C), vapor pressure deficit (VPD) (s; kPa), Leaf Area Index (LAI) (t; m^2 m^{-2}). On the SOM-planes referring to VOC fluxes (a-l), the highest emission rates are represented by dark red whereas the highest deposition rates are represented by dark blue. On the SOM-planes referring to all other physiological (n-p), environmental (q-s), and structural (t) parameters the lowest measured values (approaching zero) are dark blue and the highest are dark red.

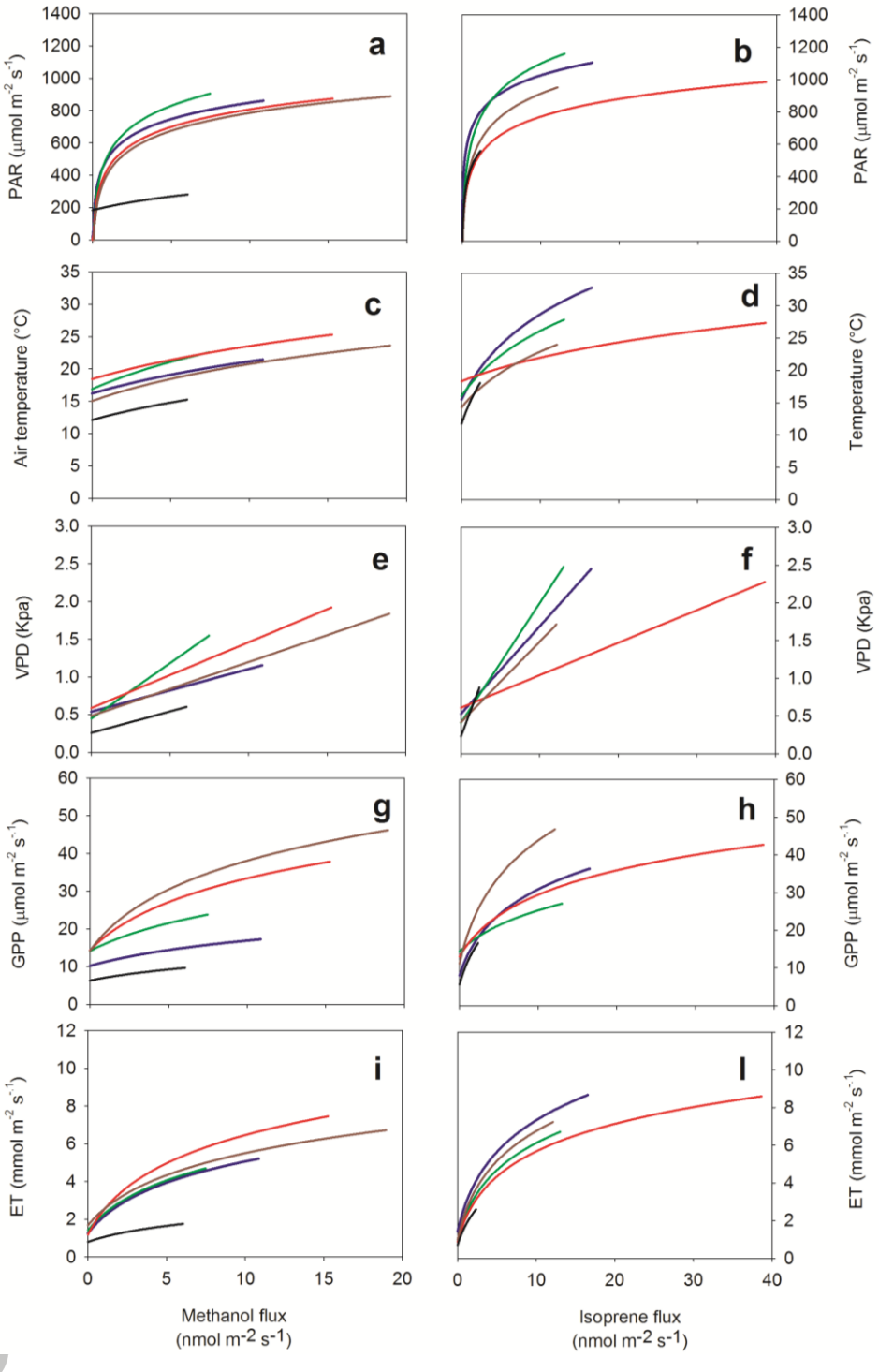

Figure 3. Relationships between methanol (a, c, e, g, i) and isoprene fluxes (b, d, f, h, l) and photosynthetic active radiation (PAR), air temperature, vapor pressure deficit (VPD), gross primary production (GPP), evapotranspiration (ET) during the daytime hours (7:00-20:00). Different colors are the best fitting lines for data collected in different months: blue = June, green = July, red = August, dark brown = September and black = October.

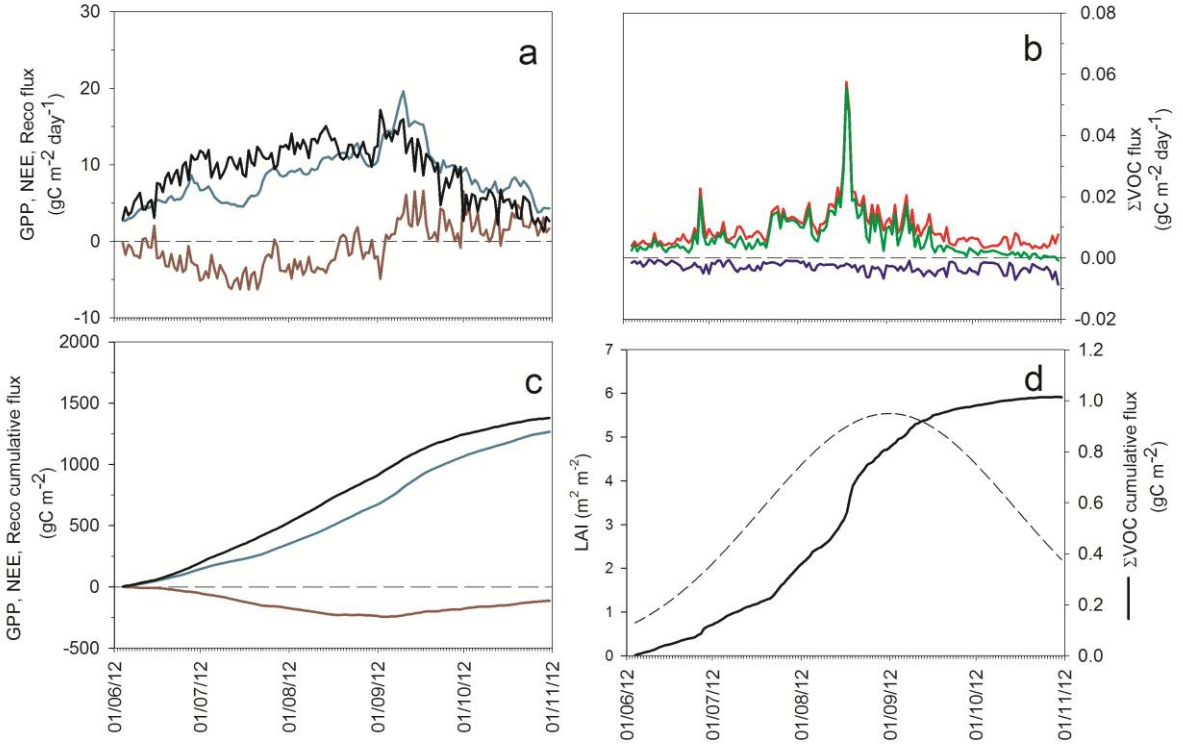

Figure 4. Seasonal variation (from 4 June to 31 October 2012) of daily (a) and cumulative (c) amount of carbon accounted as: gross primary production (GPP) (black line), net ecosystem CO_2 exchange (NEE) (blue lines) and ecosystem respiration (RECO) (dark red line). Daily amount (b) of carbon only emitted from the poplar plantation in the form of VOC (red line), only deposited to the poplar plantation in form of VOC (blue line) and the net amount of carbon resulting from the difference (Δ) between the carbon emitted – carbon deposited in form of VOC (green line). Cumulative sum of carbon emitted in the form of VOC along with continuous time-series of LAI values (d) is also shown.

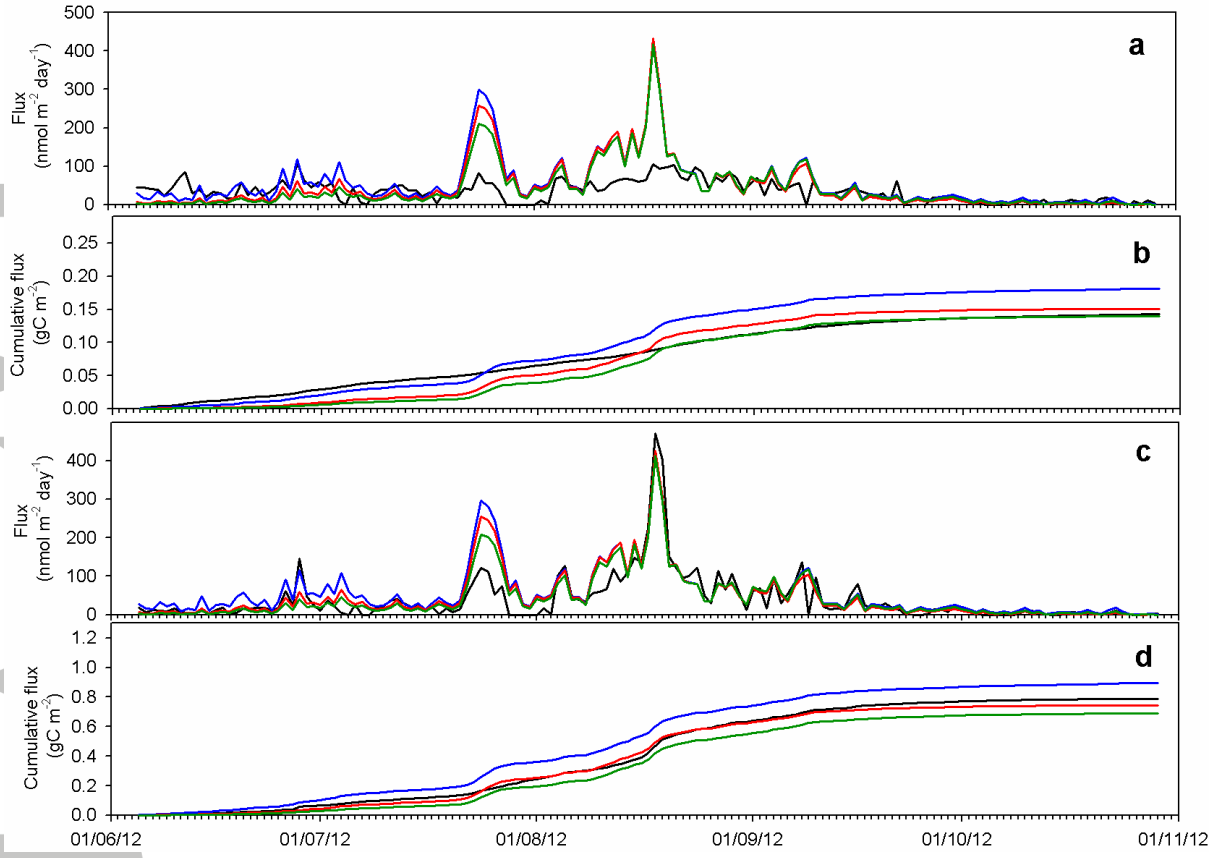

Figure 5. Daily sum of half-hourly flux emissions of methanol (a) and isoprene (c) and the cumulative sum of the carbon emitted as methanol (b) and isoprene (d) of observed flux values (black lines) when applying: i) a constant value of Basal Emission Factor (BEF) to Model of Emissions of Gases and Aerosols from Nature (MEGAN) (blue lines); ii) a dynamic value of BEF to MEGAN based on the seasonal variation of GPP (red lines); and iii) a dynamic value of BEF to MEGAN based on the seasonal variation of LAI (green lines).

Summary

• Some reactive volatile organic compounds (VOC) (especially isoprene) emitted in the atmosphere from leaves of widespread fast-growing woody bioenergy crops play a key role in climate forcing and local air quality.

• Eddy covariance VOC emission and deposition fluxes were monitored in a 'coppiced' poplar plantation during an entire growing season and their complex interactions with climatic and physiological variables also including canopy structural traits were explored by using the Self-Organizing Map (SOM).

• Rapid development of a canopy (and thus of Leaf Area Index, LAI) was associated with high methanol emissions and high rates of gross primary production (GPP) since the beginning of the growing season, while the onset of isoprene emission was delayed.

• The highest emissions of isoprene, and of isoprene photoxidation products (methyl vinyl ketone and methacrolein, i_{ox}) occurred on the hottest and sunniest days, when also GPP and evapotranspiration were highest and formaldehyde was significantly deposited.

• The accuracy of methanol and isoprene emission simulations with the MEGAN model increased by **applying** a function to modify their basal emission factors, accounting for seasonality of GPP or LAI.